


Winter 2018

# Regional Sea Level Rise Along the United States Coasts

Alessandra G. Burgos  
*Old Dominion University*

Follow this and additional works at: [https://digitalcommons.odu.edu/oeas\\_etds](https://digitalcommons.odu.edu/oeas_etds)

 Part of the [Climate Commons](#), and the [Oceanography Commons](#)

---

## Recommended Citation

Burgos, Alessandra G.. "Regional Sea Level Rise Along the United States Coasts" (2018). Master of Science (MS), thesis, Ocean/Earth/Atmos Sciences, Old Dominion University, DOI: 10.25777/kj2n-ny17  
[https://digitalcommons.odu.edu/oeas\\_etds/15](https://digitalcommons.odu.edu/oeas_etds/15)

This Thesis is brought to you for free and open access by the Ocean, Earth & Atmospheric Sciences at ODU Digital Commons. It has been accepted for inclusion in OEAS Theses and Dissertations by an authorized administrator of ODU Digital Commons. For more information, please contact [digitalcommons@odu.edu](mailto:digitalcommons@odu.edu).

**REGIONAL SEA LEVEL RISE ALONG THE UNITED STATES COASTS**

by

Alessandra G. Burgos  
B.S. May 2016, Rutgers University

A Thesis Submitted to the Faculty of  
Old Dominion University in Partial Fulfillment of the  
Requirements for the Degree of

MASTER OF SCIENCE

OCEAN AND EARTH SCIENCES

OLD DOMINION UNIVERSITY  
December 2018

Approved by:

Benjamin Hamlington (Co-Director)

John Klinck (Co-Director)

Tal Ezer (Member)

## ABSTRACT

### REGIONAL SEA LEVEL RISE ALONG THE UNITED STATES COASTS

Alessandra G. Burgos  
Old Dominion University, 2018  
Co-Directors: Dr. Benjamin Hamlington  
Dr. John Klinck

Over the past several years, there has been several studies focused on reconstructing global mean sea level (GMSL) for the 20<sup>th</sup> century, along with projecting rates out into the future. Of greater importance for mitigation and adaptation plans, however, is the rate of local or regional sea level (RSL) rise. Ocean dynamics along with changes in Earth's gravitational field can cause RSL to deviate from the change in GMSL. During the satellite altimeter era covering the past two decades, RSL trends can be four times the global average, with much of this spatial variation due to internal climate variability. Isolating the long-term signal that may be expected to persist into the future, or from which an acceleration can be estimated, is a challenge with the short satellite record. Prior to the satellite altimeter era, tide gauges must be used to study past sea level variability. Tide gauges suffer from sampling challenges that make regional studies difficult, and as a result, there has been relatively little discussion and few comprehensive efforts on reproducing long-term RSL trends.

This work aims to determine the 20<sup>th</sup> century regional pattern of sea level rise by reducing the tide gauge data to a usable subset and taking into account the factors that cause spatial variability in trends on long time-scales. This provides an estimate of secular changes leading to RSL rise associated with anthropogenic affects. Either exacerbating or suppressing these regional trends is natural internal climate variability. By determining the frequency and magnitude of these inter-annual to decadal events, we can determine a baseline of future RSL along the East and West coast of the United states. This is an important step for mitigation and adaptation plans, since high frequency events such as storms and high tides will be coupled with

RSL rise, causing increased flooding and inundation. As such, we will determine future nuisance flooding in Norfolk, VA, arising from a combination of sea level contributors from tides to internal climate variability.

Copyright, 2018, by Alessandra G. Burgos, All Rights Reserved.

This thesis is dedicated to my younger self.  
You did it.

## ACKNOWLEDGMENTS

Thank you to my advisor Dr. Benjamin Hamlington for personally reaching out to me when I applied for graduate school, and helping me learn so much about oceanography. You have been a huge support system and I am forever grateful.

Additional thanks to the following people:

- Dr. John Klinck for your no-nonsense attitude and great stories. Thank you for your help, support, and patience,
- Dr. Tal Ezer for your probing questions to push me to question my research further,
- The whole Center of Coastal and Physical oceanography. Special thanks to:
  - Dr. Eileen Hofmann, thank you for an amazing class in physical oceanography and choosing me to be a seminar speaker,
  - Julie Morgan, thank you for helping me with all my random needs,
  - Mia Osbey, thank you for all of the fun and help,
  - Teresa Updyke, thank you for taking me out on field work to learn about HR radars,
  - Sean O'Brien, thank you for all of the IT support that you have given me,
- my fellow graduate students, especially to Lauren Sommers, thank you for helping me through graduate school and making Norfolk feel like home,
- my parents for their love and unending support,
- and a special thanks to Jack Matteucci, I wouldn't be where I am today without your support and help. Thank you for your patience in tutoring me in any physics, math, or Matlab problem that I had, and for editing my papers. You were my foundation for getting through this amazing and crazy time.

## TABLE OF CONTENTS

	Page
LIST OF TABLES.....	ix
LIST OF FIGURES.....	x
 Chapter	
1. INTRODUCTION.....	1
2. AN: OBSERVATION-DRIVEN ESTIMATION OF THE SPATIAL VARIABILITY OF 20 <sup>TH</sup> CENTURY SEA LEVEL RISE.....	5
2.1 INTRODUCTION.....	5
2.2 METHODS.....	9
2.2.1 RANDOMIZATION PROCEDURE.....	12
2.3 RESULTS.....	13
3. IC: FUTURE REGIONAL SEA LEVEL RISE ALONG THE EAST AND WEST UNITED STATES COAST.....	17
3.1 INTRODUCTION.....	17
3.2 METHODS.....	19
3.2.1 INTERNAL VARIABILITY ANALYSIS.....	20
3.2.3 RANDOMIZATION PROCEDURE.....	21
3.2.4 ANTHROPOGENIC SEA LEVEL RISE AND INTERNAL CLIMATE VARIABILITY.....	22
3.3 RESULTS.....	23
4. HF: FUTURE NUISANCE FLOODING IN NORFOLK, VA FROM ASTRONOMICAL TIDES AND ANNUAL TO DECADAL INTERNAL CLIMATE VARIABILITY.....	26



Chapter	Page
4.1 INTRODUCTION.....	26
4.2 DATA.....	27
4.2.1 TIDE GAUGE DATA.....	27
4.2.2 SEA LEVEL RISE SCENARIOS.....	28
4.3 METHODS.....	29
4.3.1 TIDAL ANALYSIS.....	29
4.3.2 INTERNAL CLIMATE VARIABILITY.....	31
4.4 RESULTS.....	33
5. DISCUSSION AND CONCLUSION.....	36
5.1 OVERVIEW.....	36
5.2 DISCUSSION.....	37
5.2.1 20 <sup>TH</sup> CENTURY SEA LEVEL RISE.....	37
5.2.2 FUTURE SEA LEVEL RISE ON THE EAST AND WEST U.S. COAST.....	38
5.2.3 NUISANCE FLOODING NORFOLK, VIRGINIA.....	39
5.3 CONCLUSIONS.....	40
REFERENCES.....	42
VITA.....	49

**LIST OF TABLES**

Table	Page
1. Global mean sea level trends from mass change fingerprints.....	16
2. Sea level datums for Sewell's Point tide gauge.....	27

**LIST OF FIGURES**

Figure	Page
1. Global mean sea level rise (Source: NASA JPL 2013).....	2
2. Regional sea level trends (Source: NASA JPL 2013).....	3
3. Location of high quality tide gauges.....	7
4. Gravitational ice melt fingerprints (Source: Thompson et al. 2016).....	8
5. Probability density function of the ‘true’ 20 <sup>th</sup> century global mean sea level (Source: Thompson et al. 2016) .....	8
6. EOF 1 and Principle component from CMIP5 models .....	11
7. 20 <sup>th</sup> century regional sea level trend map.....	14
8. 20 <sup>th</sup> century regional sea level trends from anthropogenic forces.....	15
9. 1993 AVISO data along the East and West United States coast.....	19
10. Intrinsic mode functions near Fort Lauderdale, Florida.....	21
11. Maximum and minimum sea level estimates for 2030 and 2050 on the East U.S. coast .....	23
12. Maximum and minimum sea level estimates for 2030 and 2050 on the West U.S. coast .....	24
13. Annual mean sea level at Sewell’s Point tide gauge.....	28
14. Past and future tidal estimates at Sewell’s Point.....	30
15. Predicted high tides in Norfolk, 1960 - 2050.....	31
16. Intrinsic mode functions from Sewell’s Point.....	32
17. Average flood events from sea level rise, tides, and internal climate variability in Norfolk 2018 - 2050 .....	35

## CHAPTER 1

### INTRODUCTION

Many coastal communities around the world are going to see changes in the coming years as a result of ongoing sea level rise (SLR). Adaptation and mitigation plans are going to be crucial, and how well a city can plan is going to rely heavily on how comprehensively the issue is understood. Even with significant improvements to our observing systems, the specifics of how our ocean is rising and will continue to rise, is still not well known. Understanding the suite of physical processes leading to historic, present day, and future SLR is critical for comprehending how climate change will further affect our oceans, infrastructures, and ecosystems. One of the most immediate consequences of increasing sea level, is an increase in high-tide flooding, or “nuisance flooding”. This minor flooding occurs on a small scale, generally localized to a city block, during high tide and wind-driven events, inundating and closing roads. While this flooding does not pose a major threat, it can still cause deterioration to roads and infrastructures, as well as compromise sewer systems [*Vandenberg-Rodes, 2016*]. Nuisance flooding is already a concern at many locations around the United States coastline, and these flooding events are increasing in frequency [*Dahl et al., 2017; Ezer & Atkinson, 2014; Moftakhari et al., 2015; Ray & Foster, 2016; Sweet et al., 2014; Vitousek et al., 2017*]. It will further be exacerbated due to regional SLR, and additionally may be enhanced or suppressed due to natural internal climate variability [*Sweet & Park, 2014*].

A technical report by the National Oceanic and Atmospheric Administration (NOAA) concluded that nuisance flooding has mainly been occurring with high tide coupled with climate-related SLR, land subsidence, and loss of natural barriers in locations such as Baltimore, Maryland, San Francisco, California, and Norfolk, Virginia [*NOAA, 2017*]. The Hampton Roads region in southeast Virginia approximately covers 7500 km<sup>2</sup> of low-lying coastal land surrounded on three sides by water, making it an area primed for an increase in high-tide flooding [*Kleinosky et al., 2007*]. Already there has been a 325% increase in nuisance flooding since 1960 in Norfolk, which ranks in the top ten U.S. cities with an increase in high-tide

flooding [NOAA, 2017]. More than 1.5 million people live in this area with a heavily developed coastal front in part due to Norfolk hosting the largest Naval base in the world, making this a crucial area to study [Kleinosky et al., 2007]. As the number of flood days increase and intensify with ongoing SLR, coastal populations need accurate assessments of future nuisance flooding to help shape adaptation plans. In light of this, coastal towns need accurate measurements and projections of their relative regional SLR since this is a major influence in how flooding is going to impact an area.

Over the past two decades, global mean sea level (GMSL) and regional sea level have been measured continuously from satellite altimetry providing clear evidence of global and regional SLR (Figure 1). This data has shown that coastlines around the world can differ greatly in terms of their regional SLR, with some areas having considerably higher regional sea level than GMSL, with some areas below. In reality, regional deviations from the mean can reach 50 - 100% along Earth's coastlines (Figure 2) [NASA JPL, 2013]. Several studies have reconstructed historical GMSL, but very few have looked at centennial, or 20<sup>th</sup> century, regional trends, which is key to put the altimeter record into context and determine accelerations. This is crucial for informing predictions about future SLR.

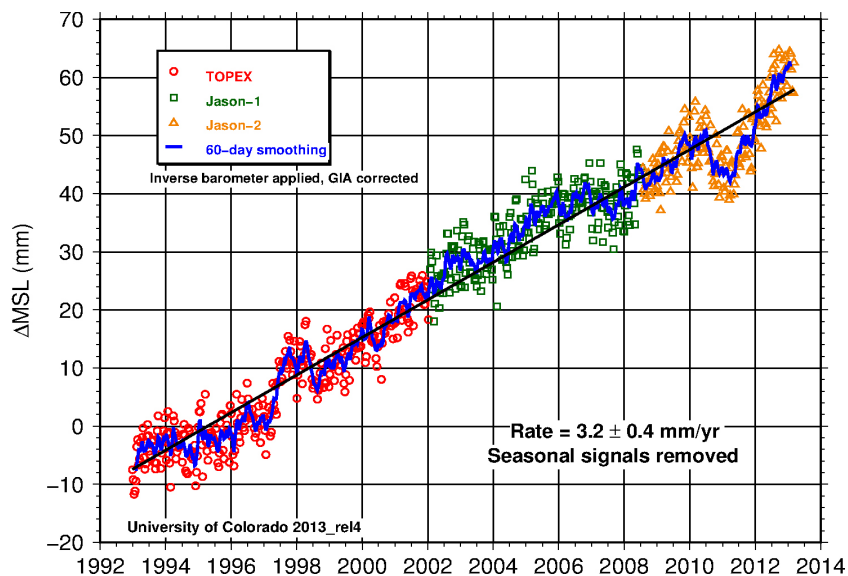


**Figure 1:** Global mean sea level rise gathered from satellite altimetry from the years 1993 to 2013 (Source: NASA JPL 2013 <https://www.jpl.nasa.gov/news/news.php?release=2013-213> )

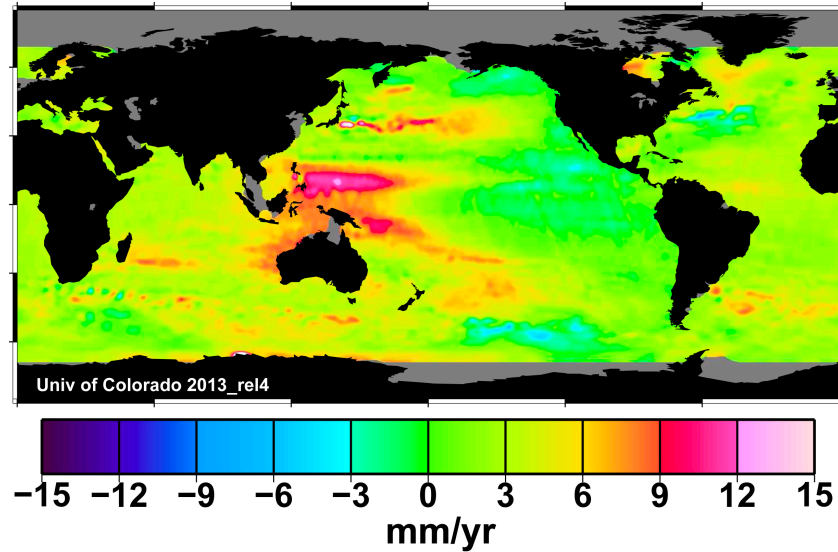


**Figure 2:** Spatial variability of regional sea level trends from satellite altimetry over the period 1993 to 2012. (Source: NASA JPL 2013 <https://www.jpl.nasa.gov/news/news.php?release=2013-213> )

Sea level has been increasing throughout the century mainly due to the ocean warming leading to thermal expansion and from the added melt sources of land glaciers [Church & White, 2011]. This is expected to continue throughout the coming decades due to the buildup of greenhouse gasses in our atmosphere trapping more heat within our troposphere. On top of this, natural internal climate variability (IC) on inter-annual to decadal time-scales will influence regional SLR [Carson *et al.*, 2015; Han *et al.*, 2013; Han *et al.*, 2016; Hu & Deser, 2013; Marcos *et al.*, 2016; Wahl & Chambers, 2016]. IC includes events such as the El Niño Southern Oscillation (ENSO), Pacific Decadal Oscillation (PDO), and the North Atlantic Oscillation (NAO), all of which can impact sea level height. Conceptually, IC acts as a lowering or rising of the sea level baseline, which can lead to an increase or decrease of nuisance flood events, or any other high frequency event. One example of how IC affects ocean height was seen in the western tropical Pacific, where sea level increased by tens of centimeters over the past few years, which was most likely due to natural decadal variability [Merrifield *et al.*, 2012]. There has been a multitude of studies to assess and quantify how specific inter-annual to decadal events could impact regional SLR [Boening *et al.*, 2012; Hamlington *et al.*, 2013, 2015, 2016a; Han *et al.*,

2016a; *Wahl & Chambers, 2016*]. However, it is the accumulation of *all* IC events on these time-scales that influences sea level height, which will affect high frequency events.

Almost all the earth system components play a role in shaping relative SLR (RSLR) on the regional scale, along with multiple feedbacks, making this a very complex issue. (Relative indicates the sea level related to the level of the land.) While there are several ways to consider the factors leading to RSLR, here the focus is on the time-scales of variability. To look at RSLR, as a function of region ( $r$ ) and time ( $t$ ), different components need to be considered, which are shown in the following equation:

$$RSLR(r, t) = AN(r, t) + IC(r, t) + HF(r, t) + LM(r, t) \quad (1)$$

Where AN refers to the secular trend associated with anthropogenic forcing (thermal expansion, and melting ice sheets), IC represents the climactic internal variability on inter-annual to decadal time-scales, HF is the high-frequency variability ranging from synoptic to annual time-scales (events like storms, seasonal heating, tides, etc.), and LM is the land motion at the coast.

In this project, the main focus will be on making a contribution to the AN and IC terms, with a case study to look at high frequency nuisance flood events in Norfolk, VA. There will not be an emphasis on the LM term due to the difficulty and uncertainty in producing accurate long term land motion estimates, which is discussed further in chapter 2. By taking an in-depth look into these 3 components, we can create better evaluations of regional RSLR over the 20<sup>th</sup> century, which will help improve future estimates of SLR along the coast, thus allowing for better assessments of future nuisance flooding. Specifically, regional sea level trends will be reconstructed over the 20<sup>th</sup> century, future regional SLR will be computed for the East and West coasts of the United States, and future nuisance flooding estimates will be calculated for Norfolk, VA. In short, improving the understanding of past, present, and future SLR is a crucial step before quality and long lasting adaption plans can be implemented.

## CHAPTER 2

### **AN: OBSERVATION-DRIVEN ESTIMATIONS OF THE SPATIAL VARIABILITY OF 20<sup>TH</sup> CENTURY SEA LEVEL RISE**

#### 2.1 INTRODUCTION

With mitigation and adaptation plans already underway in the face of sea level rise, the most critical information is in understanding how sea level varies regionally. There have been a multitude of studies to determine GMSL over the 20<sup>th</sup> century, with estimates ranging between 1.1 - 1.9 mm/yr [*Church & White, 2006, 2011; Church et al. 2004; Dangendorf et al., 2017; Hay et al., 2015; Jevrejeva et al., 2014; Ray & Douglas, 2011; Thompson et al., 2016*]. However, there has been few comprehensive studies to understand the spatial trends of RSLR over the same time-scale. To obtain historical data prior to the satellite altimeter record, tide gauge (TG) data needs to be used, which inherently has several issues. First, there is poor sampling in the ocean interior with heavy sampling along continents, leading to oceanographic and geodetic processes that vertically displace the TG. This potential vertical displacement presents an issue, as it is difficult or almost impossible to correct for vertical land motions (LM term) on long time-scales. Vertical motion due to glacial isostatic adjustment (GIA) is generally modeled and can be removed from the TG record. Beyond GIA though, there are other processes leading to vertical displacement. In these cases, GPS could be used, but the data only spans over the last two decades and studies correcting TG's for vertical land motion using GPS show that it introduces a large measure of error [*Dangendorf et al., 2017; Hamlington et al., 2016b; Wöppelmann & Marcos, 2016*]. Second, the TG network dominates the later half of the 20<sup>th</sup> century and is heavily clustered in the Northern hemisphere. Lastly, many of these individual records only span a short time throughout the century with very few gauges having extensive continuous data. The constantly changing TG network and the variable temporal and spatial sampling of oceanographic and geodetic processes is a large source of uncertainty when determining GMSL and regional RSRL from TG's.



To help combat these discrepancies, several methods have been developed to combine the TG data with modern day spatial information [Church & White, 2006, 2011; Hamlington, 2011; Hay et al., 2015; Jevrejeva et al., 2008; Ray & Douglas, 2011; Thompson et al., 2016]. Existing observations from satellite altimetry, satellite gravity, along with climate models can all be coupled with TG data. By using these different observations, better estimations of historical GMSL have been created.

Here we expand upon the work of Thompson et al. [2016] to determine how sea level has varied spatially over the last century. The goal in that study was to determine how reconstructing 20<sup>th</sup> century GMSL compared to observed TG data by using GIA and ice melt estimates, along with climate model simulations from the Coupled Model Intercomparison Project 5 (CMIP5). A few key criteria were established when determining the GMSL using TG records, since the vast majority of TG's have less than 50 years of 20<sup>th</sup> century data, making it difficult to establish longer SLR trends. In response to the sparse data, only the longest and highest quality TG records were used in the study; where high quality indicates records that are 70% complete and are minimally affected by

- 1) tectonic activity
- 2) subsidence or uplift not due to GIA
- 3) discontinuities from relocation or removal of TG's

Only 15 records met this requirement from 1901- 2000, and after taking a least-squares linear trend, this resulted in a GMSL of  $1.69 \pm 0.54$  mm/yr [Thompson et al., 2016]. Figure 3 shows the location of the TG's selected.

To determine if ocean dynamics or geodetic processes lead to these TG records to systematically differ from the true rate of GMSL, observations and simulations of spatial variability of sea level are used to estimate this likelihood. First the TG observations were corrected for GIA, which is an important step, especially when looking at centennial time scales, because the GIA can vary greatly around the globe. The TG observations with GIA corrections alone produced a new GMSL of  $1.57 \pm 0.23$  mm/yr [Thompson et al., 2016]. Another factor that needs to be taken into account is the fact that SLR resulting from land ice melt is not spatially uniform. The gravitational pull of the ice mass results in sea level to be higher in an area of ice,

and as the ice melts, sea level falls closest to the ice and rises faster than the global mean rate in the far field [Thompson *et al.*, 2016].

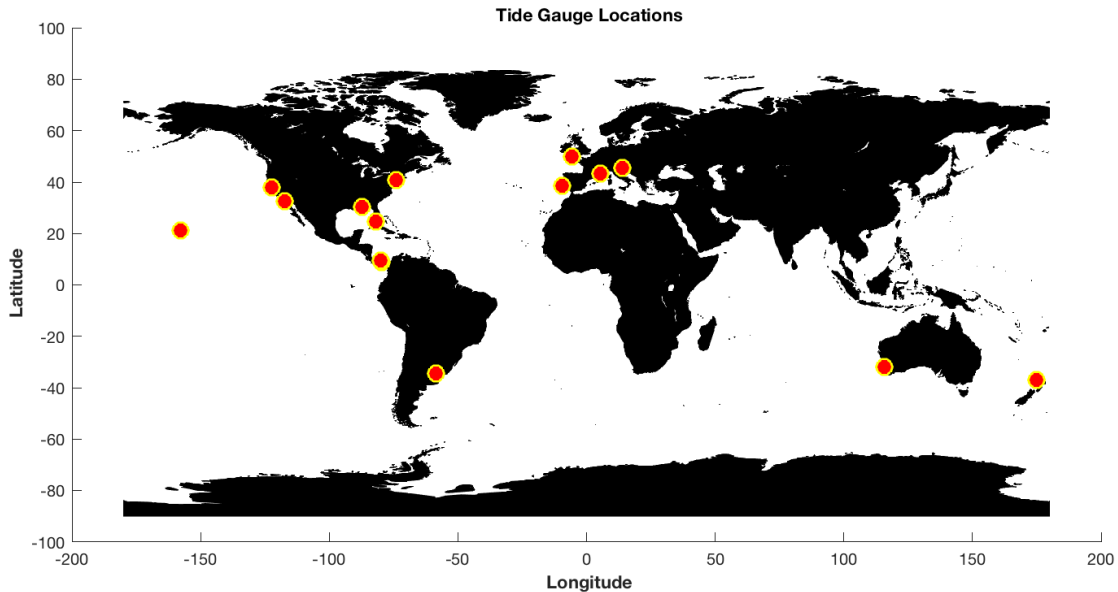


**Figure 3:** Red circles depict location of the 15 tide gauges used in Thompson *et al.*'s [2016] study.

To determine the contribution to SLR, ice sheet melt estimates, or melt fingerprints, are obtained from the Gravity Recovery and Climate Experiment (GRACE) from 2003 to 2015. These fingerprints encompass the Antarctic and Greenland ice sheets, along with 5 other geographical groupings of ice caps and glaciers (Canada, Patagonia, Alaska, Asia/ Alps, and Iceland/Russia) thought to contribute significantly to the past centuries SLR [Thompson *et al.*, 2016]. These fingerprints are shown in Figure 4 taken from Thompson *et al.*, [2016]. By combining these ice sheet fingerprints along with Empirical Orthogonal Functions (EOF's) from CMIP5 models, a sampling bias in the trends from the 15 TG records was determined (this method is discussed further in section 2.2).

Overall, the 'true' GMSL was shown to be  $1.66 \pm 0.23$  mm/year, and the 15 higher quality TG records trended towards underestimating the global trend by 0.08 mm/year [Thompson *et al.*, 2016]. Figure 5 depicts the results from this study with a probability density

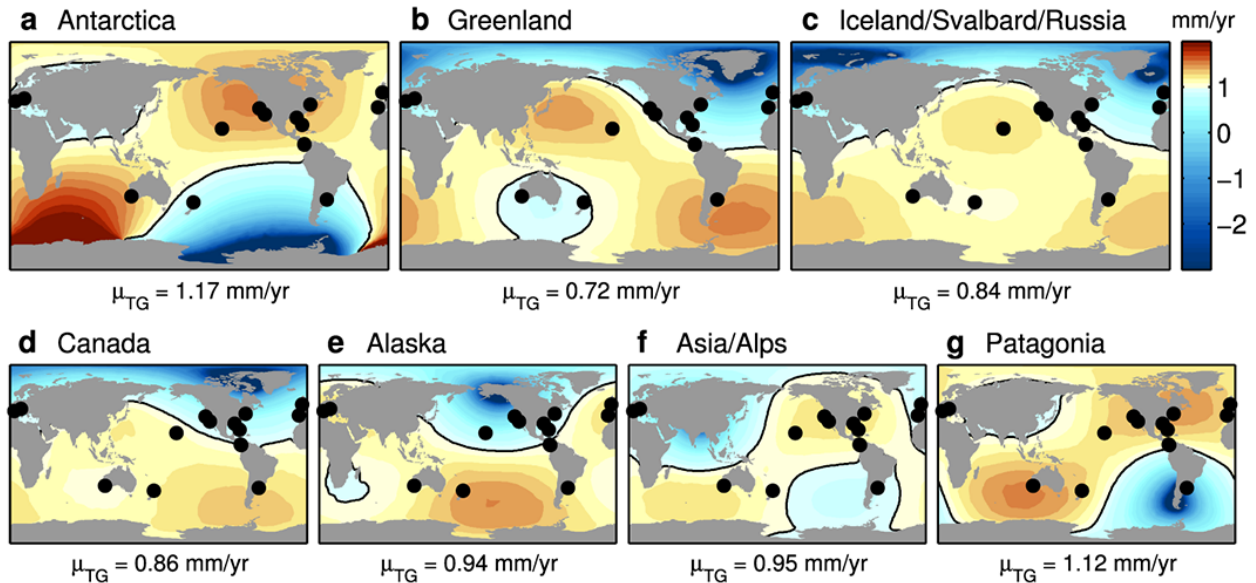


**Figure 4:** Gravitational melt fingerprints from GRACE. Each fingerprint is normalized to have a global spatial mean of 1 mm/yr, with the black line following the 1 mm/yr isoline. The mean rate at the TG's show how these locations under or overestimate the global mean associated with each melt source. (Source: *Thompson et al.* 2016 )

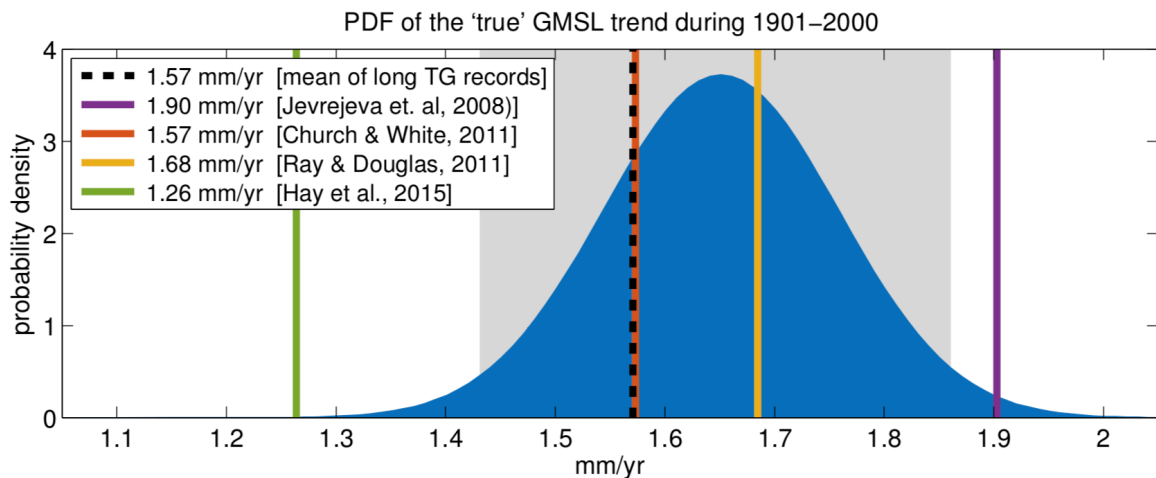


**Figure 5:** The probability density function for the 'true' rate of 20th century GMSL (blue). The gray shading shows 95% confidence intervals ( $\pm 0.23$  mm/yr) around the central value of 1.66 mm/yr.

Black dashed line shows the averaged rate from the GIA corrected TG trends.

(Source: *Thompson et al.* 2016)

function compared to the GMSL rate from several other works. It should be noted that *Thompson et al.*, [2016] states this should not be considered a definite estimate of global 20<sup>th</sup> century SLR due to the small number of TG's.

Although this approach determines the bias within longer TG records for the global mean, it does not provide much insight on the regional pattern of SLR. It does however, set up a framework for which regional trends can be computed. By building and expanding upon this method, a 20<sup>th</sup> century regional sea level trend map was created working off of the 15 TG's that were identified. These 15 gauges should be the most representative of long term change, however, there is still a standard deviation of 0.54 mm/yr amongst them. By attempting to account for the dominant processes that led to this standard deviation, we can identify the contribution made from specific processes and expand those outwards to describe the spatial trends of regional sea level on long time-scales.

## 2.2 METHODS

To account for the standard deviation seen in the 15 TG's, we consider the following equation that takes into account the larger trends over a century time-scale at the regional scale. Relative regional sea level (RRSL) trends can be computed through the following equation:

$$RRSL = GIA + IB + IM + GW + WI + OD + GC \quad (2)$$

where GIA is glacial isostatic adjustment, IB is the atmospheric loading from the inverse barometer affect, IM is the trend associated with the self-attraction and loading pattern from ice melt, GW is the regional pattern of sea level change from ground water depletion, WI is the regional trend associated with water impoundment from reservoirs and dams, OD is the regionally varying trend associated with changes in ocean dynamics and internal variability, and GC is a globally uniform trend that mostly takes into account thermal expansion. It should be noted that any other effect not taken into account in this equation will be absorbed into the GC term. These are the processes that we will be looking at that we believe contributes to the spread in the 15 TG's, or in other words, causes the sea level to vary regionally. The focus is to generate a 20<sup>th</sup> century regional trend map associated with the last 5 terms in equation 2, while also attempting to understand the uncertainties when trying to account for IB and GIA.

The first step is to remove IB trends at the TG locations. Atmospheric pressure trends can explain 25% of inter-annual sea level variability and 10-30% of recent multi-decadal sea level accelerations along the Mid-Atlantic bight and Southern New England [*Piecuch & Ponte, 2015*]. At locations north of Cape Hatters, atmospheric pressure trends can account for 50% of the variance seen in annual TG records, making this an important piece that contributes to regional sea level changes [*Piecuch et al., 2016*]. Trends associated with the inverted barometer effect were calculated using the mean of three different 20<sup>th</sup> century atmospheric pressure data sets as discussed in *Piecuch et al. [2016]*, and was removed from the 15 TG's. For GIA, generally, a single correction at each TG (on the order of -0.49 to 1.38 mm/yr) would be removed from the TG trends, but GIA estimates are uncertain and can vary, which led us to use the results from *Caron et al. [2017]*, to generate new possible solutions of GIA. This follows a Bayesian approach that provides expected GIA corrections at each TG location along with its uncertainties.

The next factors to consider are the regional trend variabilities from mass changes due to the IM (ice melt), GW (groundwater withdrawal), and WI (water impoundment) terms. These fingerprints associated with mass redistribution over Earth's surface are computed following *Adhikari et al. [2016]*. The ice melt fingerprints used are the same from *Thompson et al. [2016]*, with the other two terms, GW and WI also having associated fingerprints. In total, there are 9 fingerprints - 5 associated with glaciers, 2 with ice sheets, 1 for groundwater withdrawal, and 1 for water impoundment.

Finally, to account for the steric long-scale regional variability in association with changes in ocean dynamics, an EOF calculation of 98 CMIP5 models was computed. These models take into account the variability in the ocean temperature and salinity that may be caused by internal climate variability. The CMIP5 models themselves do not capture the exact phasing of shorter scale internal variability, i.e. ENSO, PDO etc, and due to the coarse resolution, these models cannot accurately capture mesoscale variability like strong currents and coastal processes. Because the ocean dynamic trends cannot be computed over the same time scale as the TG's, the EOF's are used to derive the dominate patterns of changing ocean dynamics to provide us with possible patterns of dynamic sea level change. Figure 6 provides an example of the first EOF and its corresponding principle component (PC). This first EOF accounts for about

26% of the total variance in the original trend maps, and the PC shows how the strength of the pattern varies with each CMIP5 model. These EOF trends are then calculated at the grid points closest to the 15 TG's. Correctly accounting for and removing the OD trend associated with the time period covered by TG trends would have been ideal, and is an important factor to keep in mind with the results of this study.

As a quick overview, we are trying to determine the magnitude of the processes that led to the standard deviation of 0.54 mm/yr amongst the 15 TG's. We have subtracted out the IB effect from each TG trend, leaving us with GIA, the mass loading terms (IC, GW, WI), and the changing ocean dynamics (computed by EOF calculations). Now the goal is to figure out how these 5 terms fit together and their resulting magnitude and spatial variability.

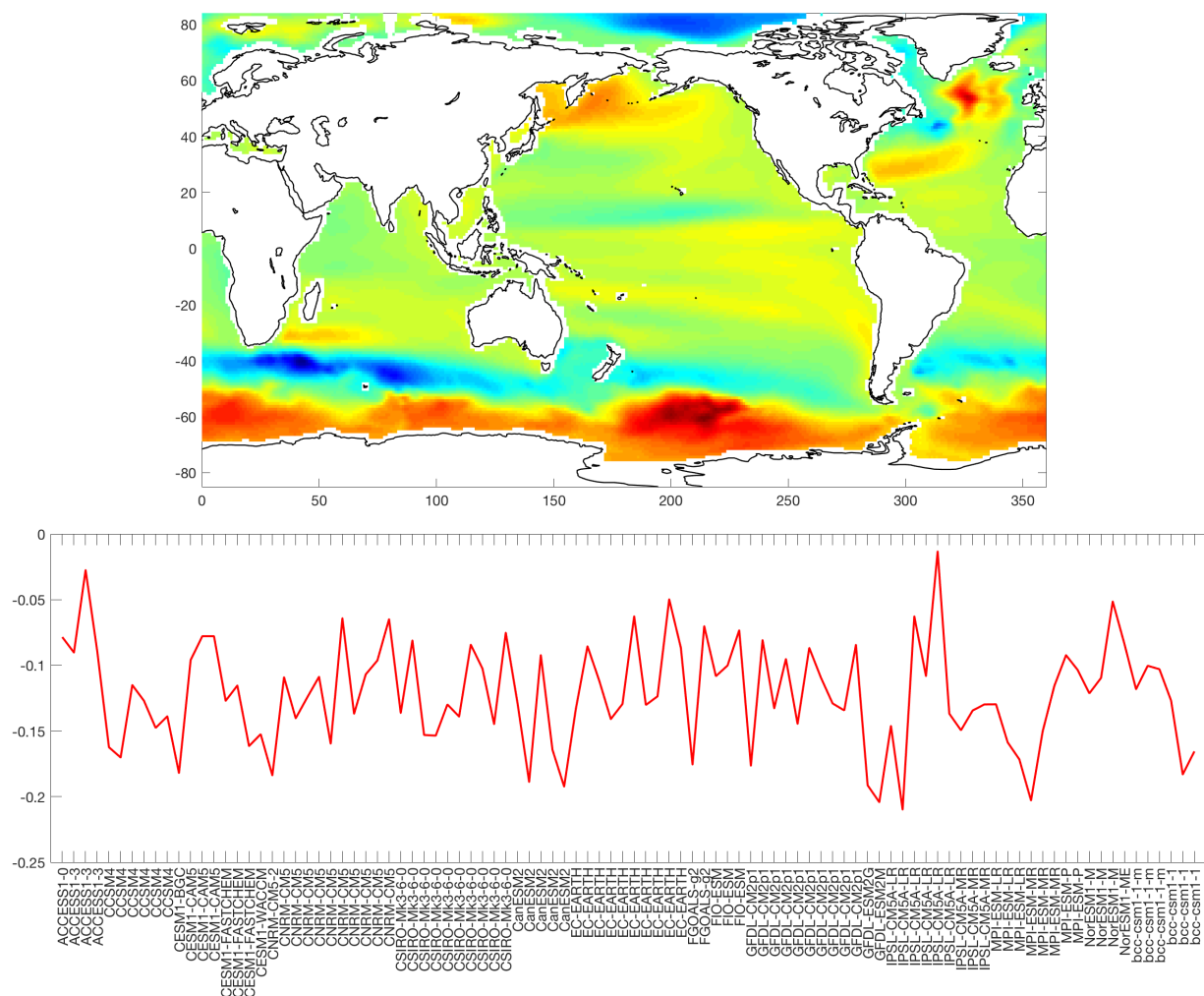


**Figure 6:** Top plot- EOF 1 calculated from the 98 CMIP5 models. Bottom plot- Accompanying principle component.

### 2.2.1 RANDOMIZATION PROCEDURE

After removing the IB trend from the 15 TG's, reducing the standard deviation to 0.52 mm/yr, a combination of GIA, amplitudes of the previously mentioned 9 fingerprints, and ocean dynamic trends need to be combined in a way to account for the rest of the variability that results in the aforementioned standard deviation. To do this, we generate random combinations of these processes. Given the 9 fingerprints, EOF's, and GIA estimates, linear combinations of these patterns with randomized amplitudes for each, are created to quantify the sampling bias in the 15 TG trends. For each one of these contributors (GIA, IM, GW, WI, OD), models for the probability of possible amplitudes for each one were determined. For GIA, these values follow a multivariate normal distribution centered on the expected value from the Bayesian framework, and account for the covariance between the GIA signal at the 15 TG locations [Caron *et al.*, 2017].

The distribution for the ice melt fingerprints are drawn from pre-defined constraints, which are briefly summarized here. For the full details, readers are referred to Thompson *et al.* [2016]. Using cryospheric observations over the 20<sup>th</sup> century, it has been gathered that the total amount of glacial melt from outside of the Greenland and Antarctica ice sheets has a 90% confidence interval of contributing 0.47 - 0.61 mm/yr [Church *et al.*, 2013; Vaughan *et al.* 2013]. Studies on Greenland glaciers show a 90% confidence interval of 0.1 - 0.19 mm/yr of melt [Gregory *et al.*, 2013], while Antarctica has an ice melt constraint of -0.2 - 0.5 mm/yr [Gregory *et al.*, 2013; Huybrechts *et al.*, 2011]. Overall, the total ice melt from all sources is constrained to be less than 1 mm/yr. Our analysis however, went beyond Thompson *et al.* [2016] to include fingerprints for GW and WI and the amplitudes for these 2 contributions were drawn from a normal distribution centered on a mean of 0.17 mm/yr and 0.16 mm/yr with standard deviations of 0.07 mm/yr and 0.1 mm/yr respectively [Lehner *et al.*, 2011; Wada *et al.*, 2012]. Finally, long-term dynamic trends are randomly generated using the EOF's from the CMIP5 trends.

Again, the GIA, IM, GW, WI, and OD estimates were randomized to create random combinations containing all 5 processes to account for the spatial variability in sea level seen in the 15 TG's. For this step, only combinations that reduced the spread in the trends of the 15 TG's are retained. Specifically, we defined a threshold to reduce the standard deviation to below 0.2

mm/yr. This cutoff is arbitrary, but after subtracting out the mean of the GIA solution, this brings the standard deviation down to 0.28 mm/yr from 0.52 mm/yr, which is part of the reason for choosing a 0.2 mm/yr cutoff.

This randomization process was repeated until  $10^4$  combinations are generated that reduced the scatter in the IB-corrected TG trends down to 0.2 mm/yr. By keeping just these combinations that reduced the scatter indicates that we are reasonably accounting for possible magnitudes of each process. With the combination of all 5 terms, we now have  $10^4$  regional trend maps. A final correction was made to the individual maps to account for the GC term in equation 2, which is representing spatially constant contributors like thermal expansion. The randomized fingerprints and EOF trends were subsampled at the TG locations and averaged. These trends were compared to GIA-corrected TG trends, and the difference between the two values was calculated, then added back onto the total map. This assures that the trend map is still following the reality of the TG's. With the completed  $10^4$  randomly generated trend maps, the average of the combinations provided us with one complete map, along with uncertainty in the individual contributors. This full map gives a result that can be compared to the TG global trend in *Thompson et al.* [2016].

### 2.3 RESULTS

The resulting 20<sup>th</sup> century regional trend map is shown in Figure 7A. Overall, we see higher trends off the coast of South Africa, extending east into the Indian ocean. Areas that have lower trends are off of the southern tip of South America and south of Greenland. The trend maps are subsampled at the TG locations and compared to the actual GIA- corrected trends at each of the 15 TG sites (Figure 7B). Blue shows the ensemble-modeled and red shows the observed GIA- corrected trends. 13 of the 15 gauges have a trend difference below 0.2 mm/year with San Diego and Key West being significantly underestimated by the trend map. Uncertainty in the full trend reconstruction is estimated and shown in Figure 7C, where areas of higher ice melt correspond with higher uncertainties.



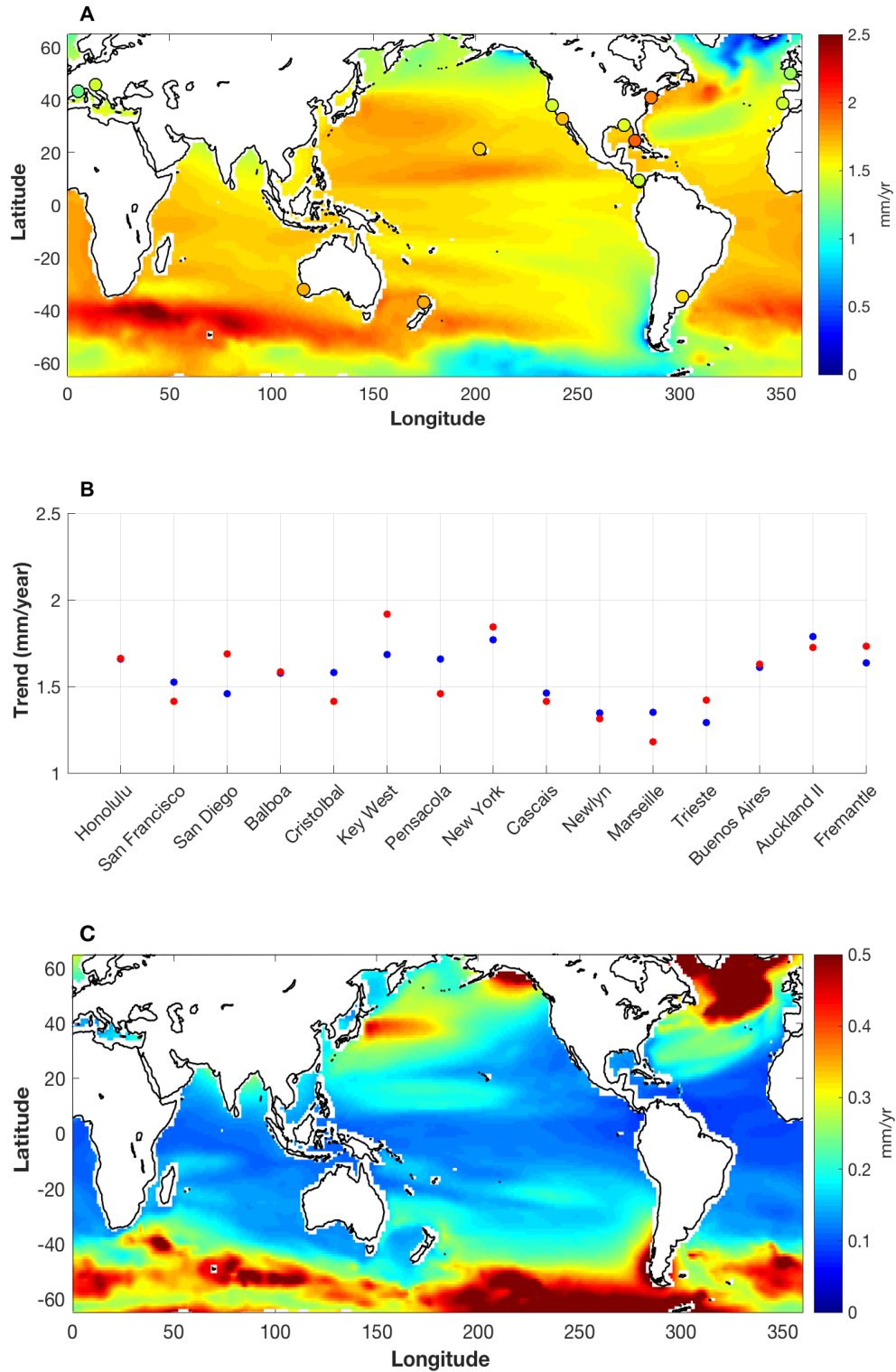


**Figure 7:** (A) 20<sup>th</sup> century trend map generated using CMIP5 EOF's to account for trends associated with the phasing of internal variability. (B) Comparison of the GIA-corrected trends (red) and the trends from A (blue) subsampled at the 15 tide-gauge locations. The mean absolute difference between the actual rates and the generated rates is 0.11 mm/year. (C) Uncertainty in the 20<sup>th</sup> century trends.

By removing the spatial variability provided by the OD term, we can isolate the IM, GW, and WI terms to see how SLR is solely affected by mass redistribution. By also forcing the trends at the TG locations to have the same mean as the GIA-corrected trends, we can include the trend represented by GC. Figure 8 shows this result, which is a combination of ice melt, ground water withdrawal, water impoundment, and the globally constant trend. This map can be thought of the sea level trends due to anthropogenic forces. Higher than average SLR is found off the U.S. West coast and in the southern Indian and Atlantic Oceans, with lower than average SLR in the South Pacific and northern parts of the Atlantic, Indian and Pacific Oceans. Each component that led to the regional SLR trends can be estimated, and are given in Table 1. The mass distribution combined, which includes IM, GW, and WI, contributes  $0.69 \pm 0.20$  mm/year to global SLR. With the GC term, this contributes another  $0.89 \pm 0.20$  mm/year leading to a final GMSL rise estimate for the 20<sup>th</sup> century of  $1.59 \pm 0.40$  mm/year. Looking at the GIA-corrected TG trends, it is shown that they underestimate the global rate by 0.09 mm/year, which is consistent with *Thompson et al.'s* [2016] study.

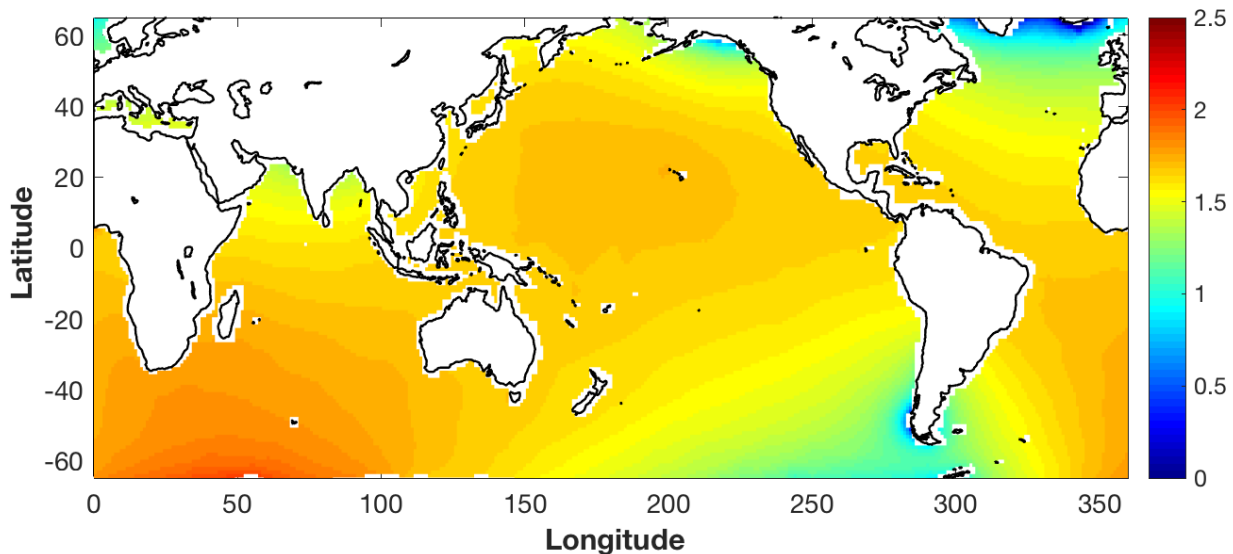


**Figure 8:** 20<sup>th</sup> century sea level trends associated with ice-melt, ground water pumping, water impoundment, and global mean thermal expansion.

<b>Contribution</b>	<b>Trends (mm/yr)</b>
Alaska	$0.08 \pm 0.09$
Canada	$0.10 \pm 0.10$
Asia/Alps	$0.13 \pm 0.09$
Iceland/Russia/Svalbard	$0.12 \pm 0.09$
Patagonia	$0.10 \pm 0.08$
Antarctica	$0.11 \pm 0.15$
Greenland	$0.13 \pm 0.13$
Groundwater Withdrawal	$0.05 \pm 0.07$
Water Impoundment	$-0.14 \pm 0.10$
Total Mass	$0.69 \pm 0.20$
Global Constant	$0.89 \pm 0.20$
GMSL	$1.59 \pm 0.40$

**Table 1:** GMSL contribution in mm/yr of each individual mass change fingerprint obtained through the randomization procedure. Uncertainty estimates represent one standard deviation as obtained by the  $10^4$  combinations generated through the randomization procedure.

## CHAPTER 3

### **IC: FUTURE REGIONAL SEA LEVEL RISE ALONG THE EAST AND WEST UNITED STATES COAST**

#### 3.1 INTRODUCTION

Natural internal climate variability (IC) plays a key role in shaping regional SLR. Natural events on several times-scales can influence ocean height. Some of these events previously mentioned include ENSO and PDO, which occur on 6-18 month and 10-30 year scales, respectively, which describes inter-annual and decadal time-scales. These natural climate phenomena produce steric changes in the ocean, including shifts in temperature and salinity. All climate events play a role in how they affect the ocean, and several studies have analyzed and described their impact on sea level [Boening *et al.*, 2012; Carson *et al.*, 2015; Hamlington *et al.*, 2013, 2016a; Han *et al.*, 2013, 2016; Marcos *et al.*, 2016; Wahl and Chambers, 2016]. The PDO has been shown to contribute up to 41% of the variance seen in regional SLR in the Pacific from 1993 to 2010 [Han *et al.*, 2016]. Also shown along the West coast of the United States, there has been suppressed sea surface height from winds associated with the PDO, making it look like sea level has changed very little along that coast [Han *et al.*, 2016].

Each climate mode impacts regional sea level differently, and these events can either be destructive or constructive with one another, leading to an enhancement or suppression of sea level height. Understanding individual modes and how they will vary in the future is an important step for creating superior SLR projections when dealing with that specific event. However, teasing apart individual IC events from sea level data is difficult, and in this case we are interested in the additive effects of all inter-annual to decadal variability. Because these modes are entwined amongst each other, it is critical to understand how events on these specific time-scales will progress in the future, either increasing or decreasing SLR. For instance, the effects from a strong storm could be amplified or suppressed depending on the phase of the total climate variability at that time. This indicates the importance for planning and mitigating purposes to determine potential future phasing of how these events will fluctuate, and combined

with regional SLR estimates, determine a baseline of future sea level along the East and West U.S. coastline.

To determine spatially how these climate events will persist into the future, an empirical mode decomposition (EMD) will be performed on available satellite altimeter data. The EMD acts as a filter and separates the natural climate signals into Intrinsic Mode Functions (IMFs) without leaving the time-domain. The assumption is that data must be composed of simple intrinsic modes of oscillations [Molla *et al.*, 2005], where the EMD will separate these oscillatory patterns into high and low frequencies. This non-linear method has been proven useful for extracting natural climate signals, and allows for inter-annual and decadal modes to be isolated from higher frequency data such as tides and seasonal cycles [Ezer, 2013; Ezer *et al.*, 2016; Molla *et al.*, 2005]. Performing this analysis on AVISO satellite data of sea level height provides a different way to approach determining IC since generally tide gauge data would be used [Cheng *et al.*, 2017; Ezer, 2013; Kenigson & Han, 2014]. By using this technique instead, it has large implications for not being reliant on the TG network, which as thoroughly discussed in chapter 2, has many issues.

One of the drawbacks of using AVISO data however, is that altimeters have difficulty in the coastal zones and data is generally flagged and discarded 10 - 50 km from shore depending on the specific instrument and local morphology, and so it is not fully applicable at the coastline [Cipollini *et al.*, 2017]. This poses a critical issue when trying to blend together TG and altimetry data, where most studies simply compare rates in different areas [Cipollini *et al.*, 2017]. Also, there are fundamental differences between the two measuring systems, where TG's are relative to Earth's crust and subject to vertical displacements, while satellite altimetry is relative to the geoid. In spite of this, a study by Vinogradov & Ponte [2011] shows that with lower frequency climate events, there is significant agreement between TG's and altimetry data. On inter-annual variability time-scales, the majority of the TG sites across continents agreed within 20% of the altimeter data, with larger variability on the West coast of United States compared to the East coast [Vinogradov & Ponte, 2011]. As the climate variability becomes larger in scale and longer in time, these events should be mostly controlled by nonlocal coastal affects [Vinogradov & Ponte, 2011]. This supports that we can reasonably infer what is occurring at the coast from the

nearest altimeter data point for inter-annual to decadal time-scales. With the results from 2.3, Figure 8, the anthropogenic map of SLR throughout the 20<sup>th</sup> century can be used to create linear projections out to the year 2030 and 2050. Combined with IC projections, a range of future SLR can be created for those years along the U.S. coastlines.

### 3.2 METHODS

AVISO altimetry monthly data was gathered from 1993 - 2016 at a  $1/4^\circ$  resolution along the East and West coast of the U.S., with the data isolated along each coastline. Figure 9 provides an example of the AVISO data averaged over 1993 sampled along the East and West coast.

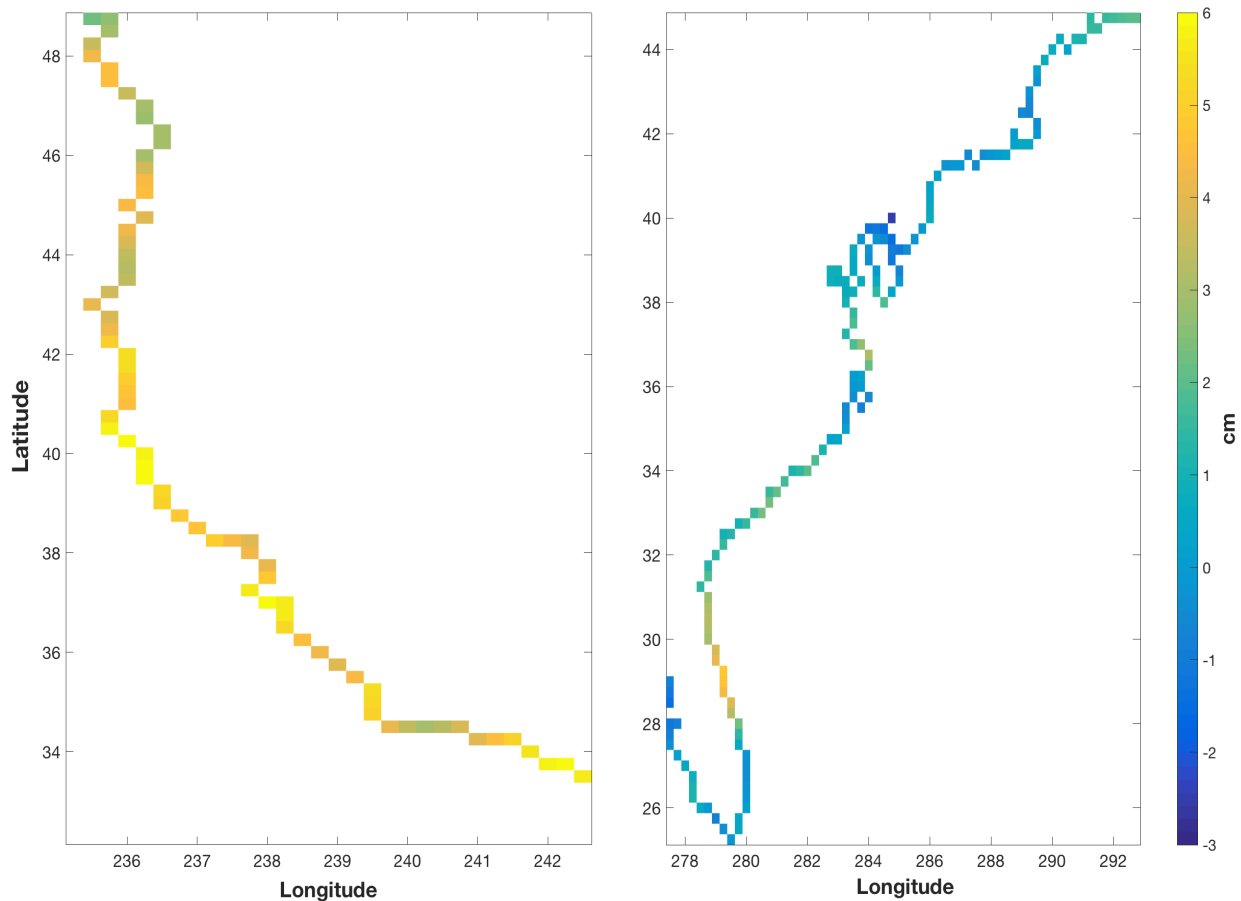


**Figure 9:** Sample of the AVISO satellite altimetry data of sea level height in cm along the West coast of the United States (left) and the East coast (right). Data averaged over the year 1993. Resolution is at a  $1/4^\circ$ .

### 3.2.1 INTERNAL VARIABILITY ANALYSIS

To distinguish the different frequencies of events in the sea level record, an EMD was performed on the AVISO data from each cell that bordered the U.S. coastline. This resulted in a range of 6-8 IMFs. These IMFs do not represent or show individual IC events, like ENSO, but instead shows the combined signals of IC on the order of a specific time-scale, from high frequency events (tides and seasonal cycles), to low frequency ones (multi-decadal events, or increasing sea level height). Each IMF series along the coast varies greatly in terms of its oscillation pattern. Figure 10 provides a sample of one of the IMF series from a coastal point along the East coast near Fort Lauderdale, Florida. This specific coastal cell shows 7 IMFs, which was the most common number obtained from the EMD.

From the resulting IMFs, we are interested in modes that show inter-annual to decadal variability, and these time-scales can be specified based on how many maxima occur in the oscillations. This was determined by the following criteria:

- 1) Inter-annual events on the order of 5 years: 7-16 maxima
- 2) Inter-annual events on the order of 10 years: 3-7 maxima
- 3) Decadal events on the order of 20 years: 1-3 maxima

This can be seen in figure 10 where the fourth to sixth IMFs follow these 3 different categories. Depending on how many resulting IMFs a coastal cell had from the EMD, and based on the above criteria, anywhere from 2 - 5 modes would be kept for further analysis. The higher frequency IMFs are not used since this describes annual variability and the uncertainty is greater for using this AVISO data to represent the coast. The last, or very low frequency IMF was also omitted (e.g. IMF 7 in Figure 10) because it represents the continuously increasing SLR and would be redundant when combined with the SLR projections [*Chambers, 2015*]. To actually use the selected IMFs, we are assuming that the same magnitude of IC will occur in the future as it has been occurring in the past. Because we cannot conclude that this variability will repeat itself exactly, we introduce a randomization procedure to provide different possibilities of how these internal variabilities could be combined and applied to in the future.

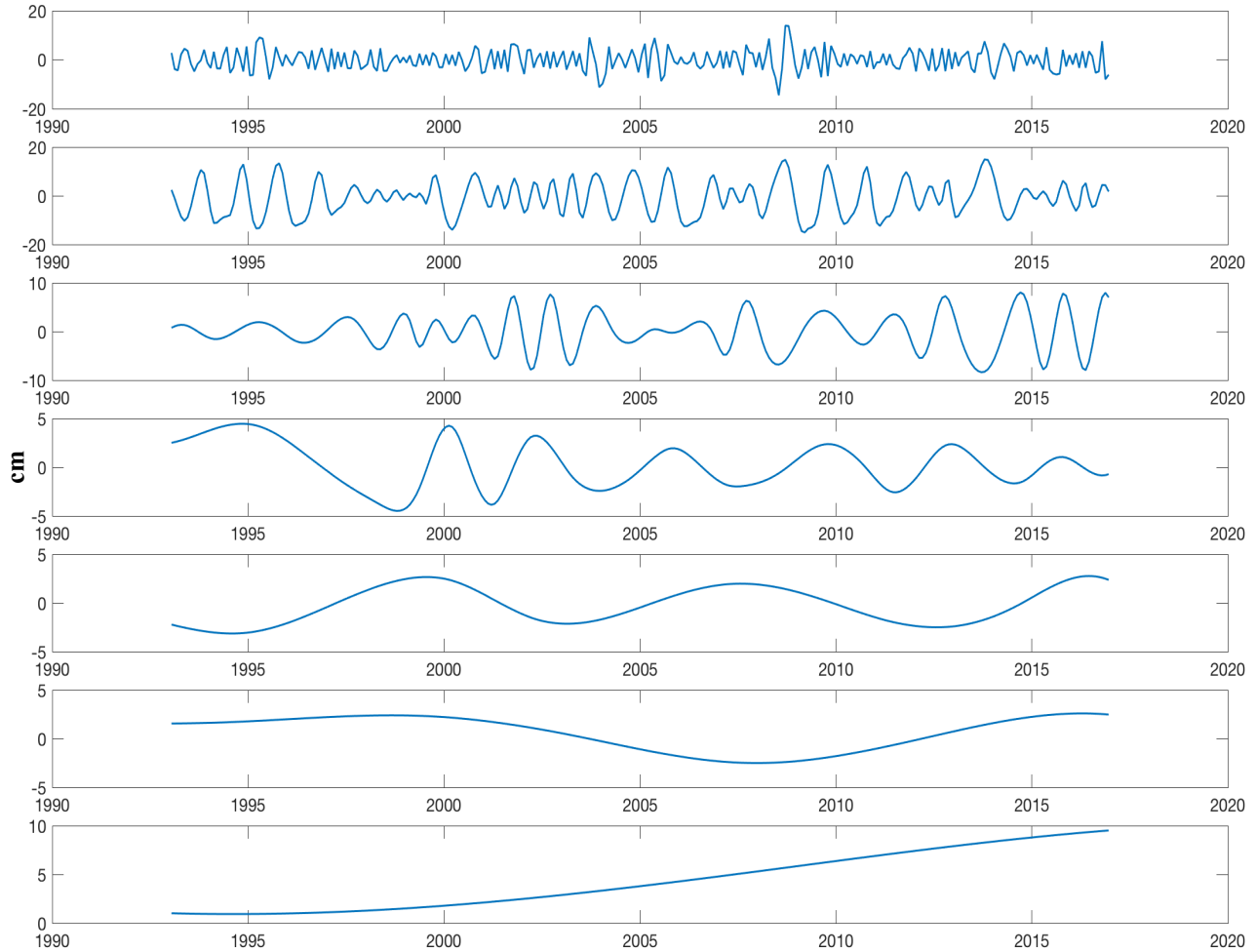


**Figure 10:** Intrinsic Mode Functions from the EMD on a spatial cell near Fort Lauderdale, Florida. Data is in mm. The top three plots indicate signals on the order of annual variability. The next two show inter-annual variability, plot 6 showing decadal variability, and the last one at multi-decadal time-scales.

### 3.2.3 RANDOMIZATION PROCEDURE

We are only interested in creating a new time series composed of internal variability for the future years beyond the observed AVISO data, which is from January 2017 to December 2050. With an IMF series for each spatial cell along the coast, the selected IMFs had randomized years extracted to create a new time-series of 34 years. To capture potential phasing of the signals, different time pieces were derived from each IMF that met the criteria as previously mentioned. More specifically, for the IMFs that met the first criteria, random 5-year segments



were taken out of that specific mode to create a new synthetic 34-year long time-series. The same was done for the IMFs that met criteria 2 and 3, where 10 and 20 year segments were extracted, respectively. With the new randomized time-series, they were added together, smoothed to remove discontinuities, and the mean subtracted. By adding together all of the modes, this provides a robust estimate of all inter-annual to decadal variability, and multiple modes (or IMFs) are needed to quantify the physical climate variability [Chambers, 2015]. This time-series now represents possible natural internal sea level height variability on the order of inter-annual to decadal time-scales. Instead of randomizing this once, the processes was repeated 1,000 times for every cell along the coastlines. This left us with 1,000 iterations of possible IC for each coastal cell along the East and West U.S. coast.

#### 3.2.4 ANTHROPOGENIC SEA LEVEL RISE AND INTERNAL CLIMATE VARIABILITY

Sea level trends due to anthropogenic causes are seen in the results section of chapter 2 (2.3, Figure 8). These trends around the East and West coast of the U.S. were isolated along the coastline and re-gridded to match the high resolution grid of the AVISO data. For reference, the anthropogenic trend map was based off of the CMIP5 grid, which follows a  $1^\circ \times 1^\circ$  resolution. The sea level trend data was then interpolated to follow the same contours along the coastline as was illustrated in Figure 9. This was necessary to effectively combine the anthropogenic sea level trend data with the IC data at each cell location. It should be noted that with the re-gridding of the anthropogenic map, it may lead to a certain amount of uncertainty in the following analysis, and its effectiveness at using that data along the coastlines.

With the anthropogenic data isolated to the coastlines, the trends were linearly extended out to 2030 and 2050 relative to 2016. More simply put, these trends were extended out 14 and 34 years to provide estimates of SLR for 2030 and 2050, respectively. To determine how IC could play a role, the maximum and minimum value of the 1,000 IC iterations across coastal cells were taken for the averages of 2030 and 2050. With the maximum and minimum IC value for every cell along both coastlines, the anthropogenic trends were added on. This provided a maximum and minimum SLR map due to internal climate variability and 20<sup>th</sup> century SLR trends for 2030 and 2050.

### 3.3 RESULTS

The resulting map for the East coast is shown in Figure 11, and the West coast is shown in Figure 12. The top plots show the minimum (left) and maximum (right) map for the year 2030. The same is shown on the bottom except for the year 2050. These values represent minimum and maximum SLR estimates relative to 2016. The projected anthropogenic trends only contribute around 2.16 – 2.28 cm (2.2 cm) for 2030 and 5.25 – 5.6 cm (5.4 cm) for 2050 along the East (West) coast.

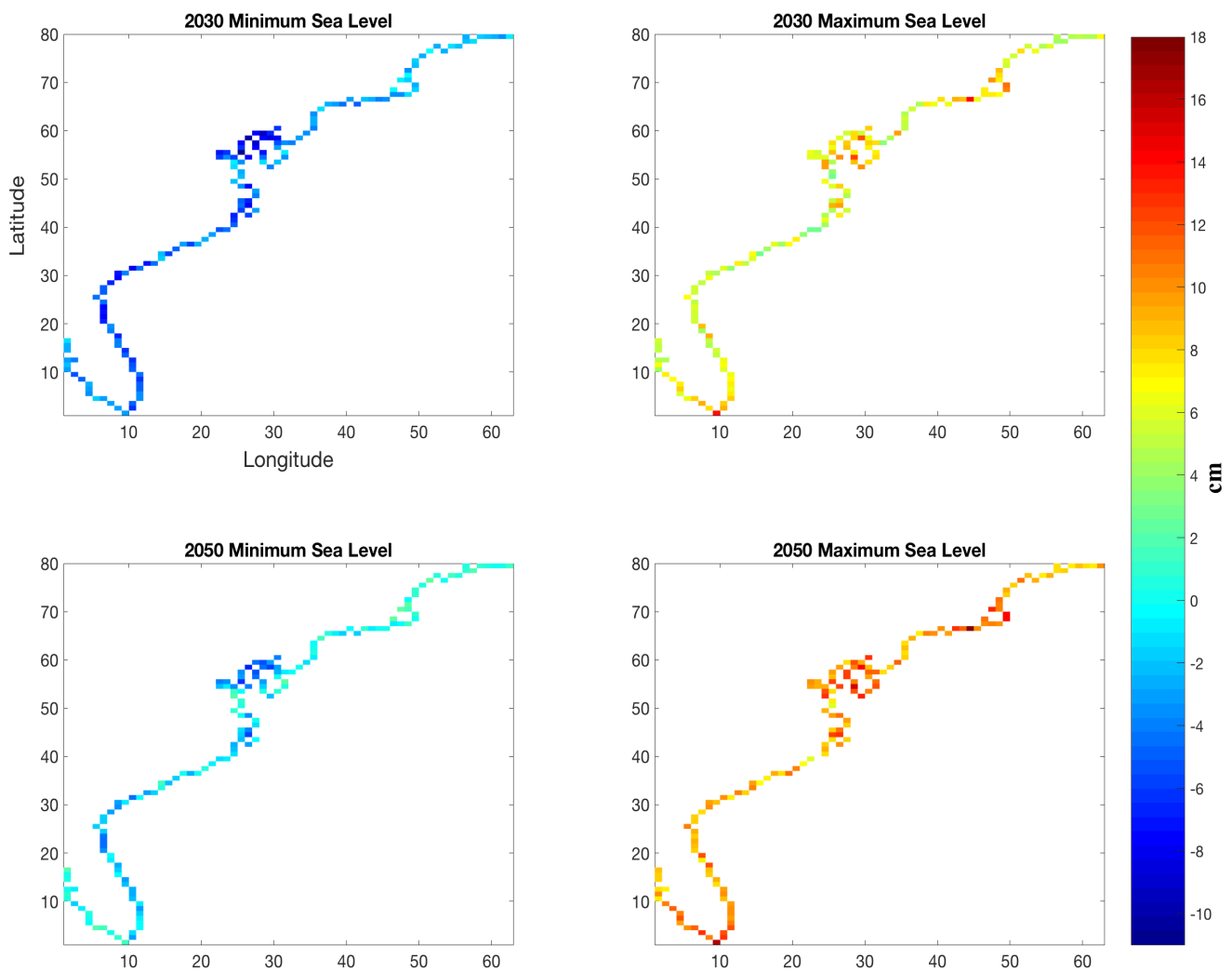


**Figure 11:** Future sea level rise along the U.S. East coast based off of the 2016 sea level height from internal climate variability estimates combined with 20<sup>th</sup> century anthropogenic sea level rise trends.

Units are in cm. Top left: Minimum sea level rise for 2030; Top right: Maximum sea level rise for 2030; Bottom left: Minimum sea level rise for 2050; Bottom right: Maximum sea level rise for 2050

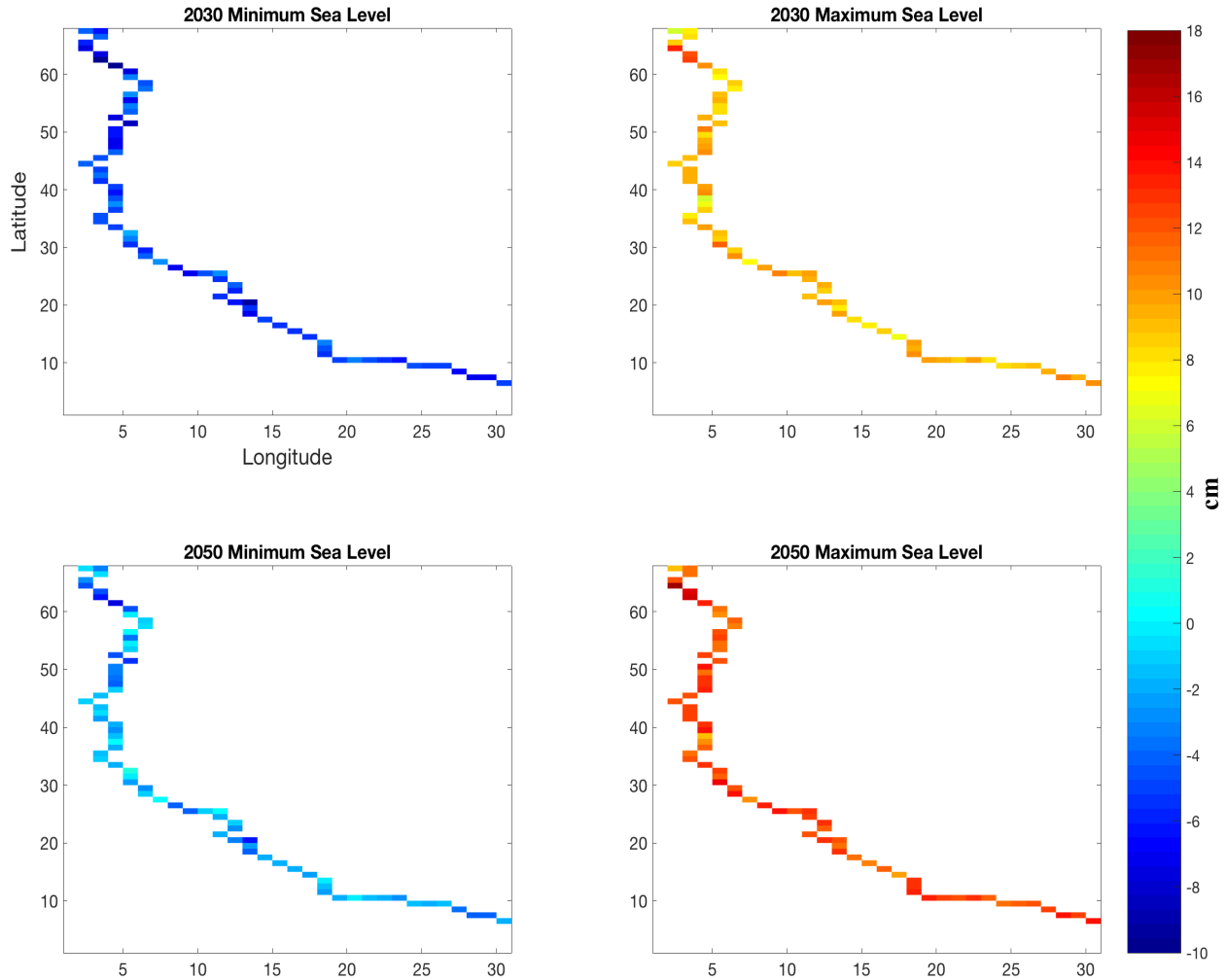


**Figure 12:** Future sea level rise along the U.S. West coast based off of the 2016 sea level height from internal climate variability estimates combined with 20<sup>th</sup> century anthropogenic sea level rise trends. Units are in cm. Top left: Minimum sea level rise for 2030; Top right: Maximum sea level rise for 2030; Bottom left: Minimum sea level rise for 2050; Bottom right: Maximum sea level rise for 2050

It is clear that with the small linear sea level trend, the internal variability is playing the largest role in changing sea level. For both the East and West coastlines, the minimum contribution to sea level rise in 2030 and 2050 ranges around -10 – 2 cm. Although it is not expected for sea level to drastically decrease in the future along the entire coastline, this resulted due to the randomization procedure combining IC events in such a way that there was a negative impact on sea level overall. The highest SLR is expected in 2050 on both coasts as anthropogenic effects continue to increase the ocean height from the main contributing factors of ice melt and thermal

expansion. There is a range on the East coast from 3 – 14 cm for the year 2030 and 7 – 18 cm in 2050. The range displayed on the West coast shows 6 – 14 cm in 2030 and 11 – 18 cm in 2050. The East coast shows more ‘hot-spots’, while the West coast shows more uniform values along the coastline. This is in part due to the small regional variability in the anthropogenic sea level trends on the West coast, and possibly because IC events such as ENSO and PDO show up more readily in the satellite data leading to more consistent trends. The East coast also has a much stronger dynamic impact due to the Gulf Stream, which is discussed further in *Ezer* [2017].

Comparing select locations along the coasts in the maximum sea level maps to other studies [*Boon et al.*, 2018; *Hu & Deser*, 2013; *Sweet et al.*, 2017; *Telbaldi et al.*, 2012] shows mixed results. Compared to *Hu & Deser* [2013], who evaluated the impact IC has on SLR, the regional internal variability estimates presented here on the East coast are in the same range as their regional trend values. The West coast trends here, however, are overestimates in locations such as San Francisco and Los Angeles, CA. For the other studies, in general for both coasts, the maximum sea level scenarios for the year 2030 follows relatively close to the intermediate to intermediate-high SLR scenarios from the studies of *Sweet et al.*, [2017] and *Telbaldi et al.*, [2012], or the ‘linear’ trend in *Boon et al.*, [2018] give or take 2 – 3 centimeters, while for 2050, the presented results are significantly underestimated. Comparing solely to the *Boon et al.* [2018] study, however, the results for the West coast show locations that are overestimating the trends such as in San Diego, CA or South Beach, OR for 2030 and 2050. In general however, it is reasonable that the 2050 maximum trends are underestimates due to the conservative linear 20<sup>th</sup> century sea level trends being used. If accelerations were taken into account, then maximum and minimum values would expect to increase. None of the minimum sea level results here are comparable to studies, and are a severe underestimate of realistic future trends.

## CHAPTER 4

### ***HF*: FUTURE NUISANCE FLOODING IN NORFOLK, VA FROM ASTRONOMICAL TIDES AND ANNUAL TO DECADEAL INTERNAL CLIMATE VARIABILITY**

#### 4.1 INTRODUCTION

One of the largest contributors to nuisance flooding is high frequency events, which can range from unpredictable wind-driven events to predictable tides on the order of days or hours. As SLR continues, instances of nuisance flooding are going to increase [*Dahl et al.*, 2017; *Moftakhari et al.*, 2015; *Ray and Foster*, 2016; *Sweet et al.*, 2017; *Sweet & Park*, 2014; *Vandenberg-Rodes et al.*, 2016; *Vitousek et al.*, 2017;]. This flooding can also be exacerbated by changes in ocean circulation, such as variations in the Gulf Stream, and from natural internal climate variability (IC), all of which affect sea level [*Carson et al.*, 2015; *Ezer*, 2016; *Ezer et al.*, 2013; *Ezer and Atkinson*, 2017]. As mentioned in Chapter 1, Norfolk, Virginia is a critical area to study due to the large coastal population, and hosting the largest naval base in the world. To determine how the Hampton Roads area in the future will be further impacted by nuisance flooding, our work will extend the methodology from *Ray and Foster* [2016] who determined future nuisance flooding in Boston by looking at tidal predications combined with long-term SLR scenarios. The first scenario was a linear 20<sup>th</sup> century rate, which was taken to be a very conservative estimate. The second one took into account the “Intermediate - High” scenario from the U.S. National Climate Assessment and adjusted for local conditions. By combining the tidal predictions with the two different scenarios of SLR, an estimation of nuisance flooding in Boston in the future was determined. They showed that in Boston, nuisance flooding was seen from tides alone beginning in 2011, and in the future, the number of events heavily increased.

*Ray and Foster's* [2016] method solely used tidal predications and SLR scenarios to predict the future nuisance flooding in Boston. This is very specific to each port, where each tidal analysis needs to be adjusted for the local area. A key element that is missing from their work are the predicted affects from IC. This chapter looks in detail how nuisance flooding in Norfolk, VA may change in the future due to rising seas coupled with tides and IC. The first analysis for

Norfolk is modeled after *Ray and Foster* [2016] with tidal data specific for Norfolk. A second analysis looks at the coupled affects from tides and IC on annual to decadal time-scales.

## 4.2 DATA

### 4.2.1 TIDE GAUGE DATA

The Sewell’s Point tide gauge is located north of downtown Norfolk (36.947, -76.330). The record spans from 1927 – 2016 and is 99% complete. The sea level datums for this station are provided in Table 2, as determined by NOAA for the epoch 1983 to 2001.

<b>Table 2. Sea Level Datums at Norfolk for Epoch January 1983 – December 2001</b>		
Datum	Height (cm) relative to station datum	Height (cm) relative to MSL
Nuisance Flood Level	270.6	95.8
MHHW - mean higher high water	217.6	42.8
MHW - mean high water	211.4	36.6
MSL - mean sea level	174.8	0.0
MLW - mean low water	137.4	-37.4
MLLW - mean lower low water	133.6	-41.2

**Table 2:** Sea level datums for Sewell’s Point (Source: NOAA’s Tides and Currents <https://tidesandcurrents.noaa.gov/datums.html?id=8638610> )

The annual sea level height data taken from the Permanent Service for Mean Sea Level (PSMSL) had the mean during the epoch removed to provide Figure 13. The annual instead of monthly mean sea level data was used to smooth out daily or monthly extrema, such as daily flood events, to isolate the contribution of tides alone to nuisance flooding events. Taking a least-squares linear fit yields a RSLR of  $4.6 \pm 0.29$  mm/year. The nuisance flood level is determined by NOAA’s Weather Forecast Office (NFO) at 53 cm above the MHHW [*Sweet et al.*, 2014]. This flood level is an empirical threshold, which varies from city to city depending on how the

flood waters affect the respective area. By using this threshold, however, we can determine when predicted high waters may exceed this level leading to nuisance flood events in Norfolk.

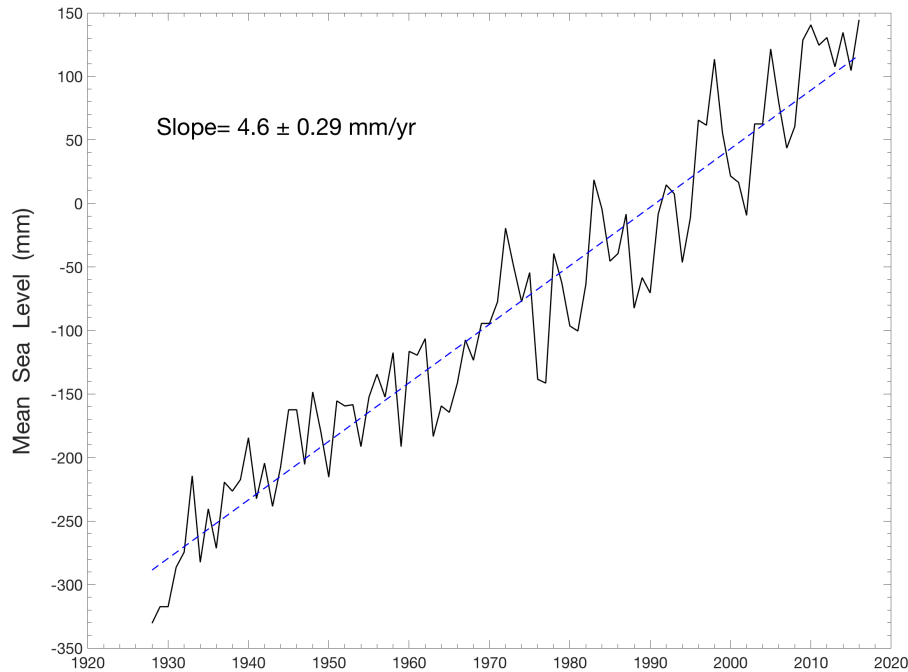


**Figure 13:** Annual mean sea level at Sewell's Point, VA from PSMSL relative to the 1983-2001 mean sea level datum from NOAA.

#### 4.2.2 SEA LEVEL RISE SCENARIOS

To create future scenarios of SLR, 3 projections were established; a low, medium, and high scenario with the observed annual record from PSMSL preceding the three projections. The medium projection follows the Intermediate-High scenario as discussed in *Telbaldi et al.* [2012] for Sewell's Point. By 2030 there is an expected 18 cm increase, and by 2050 a 40 cm increase all relative to the 2008 sea level height [*Telbaldi et al.*, 2012]. The next two scenarios are taken as a high and low end of this projection. The low scenario follows a 30 cm rise and the high scenario follows a 50 cm rise by the year 2050, again relative to the 2008 sea level height. These two limits are in line with the upper and lower bounds of projected SLR at Sewell's Point from other studies [*Boon et al.*, 2018; *Dahl, et al.*, 2017]. Although *Ray and Foster* [2016] also created

a projection in Boston by extending out the linear rate, this was seen as a conservative estimate in that study and thus was not reproduced for Norfolk. By using these three scenarios, new time series composed of the historical observations and projected future sea level heights out to the year 2050 were created. The mean sea level (MSL) found from the datum was added back into each time-series.

### 4.3 METHODS

Regional RSLR plays an important role in determining how nuisance flooding will increase in the future. Again, this can be determined from equation 1, except in this case, IC is represented from annual to decadal time-scales. All 4 terms are represented here where the HF (high frequency) term is solely represented by the tidal data. AN (anthropogenic forcing) is represented in the SLR projections along with the LM term since *Telbaldi et al.* [2012] included subsidence rates in the SLR projections. Finally, IC is considered as described below.

#### 4.3.1 TIDAL ANALYSIS

The first analysis determines the predicted nuisance flooding events in Norfolk from the combination of SLR and tides. To predict these tides at Norfolk, we estimated tidal harmonic constituents from hourly data collected over the interval 1983 – 2015. An initial spectrum of tidal residuals was used to select significant constituents up through species 10. Nearly all residual spectral lines could be accounted for by employing 88 constituents, although many of these are small and could have been neglected. As is typical, the largest constituent is the lunar semidiurnal tide  $M_2$  of amplitude 35.6 cm; it has a small seasonal modulation in both amplitude and phase. Diurnal constituents are small, the largest being  $K_1$  with an amplitude of 5.1 cm. It is known [*Flick et al.*, 2003] that the tidal range at Norfolk has slowly decreased over the course of the 20<sup>th</sup> century [*Cheng et al.*, 2017]. We have therefore analyzed historical hourly data back to 1927, and we find a secular decrease in  $M_2$  amplitude of  $-1.3 \pm 0.2$  cm/century. A corresponding decrease in phase lag is even larger:  $-4.7^\circ \pm 0.6^\circ$ /century. However, the phase time series (not shown) indicates that this large change occurred mainly between years 1950 and 1985 and the phase has not significantly changed since then. Partly owing to their somewhat erratic nature and



partly to the relatively small amplitude change, we have decided to ignore these secular changes when predicting tidal water levels into the future. The seasonal cycle in water level is appreciable at Norfolk, with mean amplitudes of the annual and semiannual constituents (over the 1983 – 2015 interval) being 6.5 and 5.0 cm, respectively. The two terms combine to produce highest water levels in late September and lowest in mid-January. These terms are included in our time series of predicted tidal high water. At the latitude of Norfolk, the 18.6-year node tide is very small, 2 mm at most, and can be ignored [Woodworth, 2012].

The tidal data created (January 1960 – December 2049) for Sewell’s Point is presented as daily data with 2 high and 2 low tidal values and is depicted in Figure 14. The high tides were isolated (the data in pink), and the annual data from the SLR scenarios starting at 1960, were added on top of the tidal values. This was done for all three scenarios, creating nuisance flood estimates from 1960 – 2050 (Figure 15).

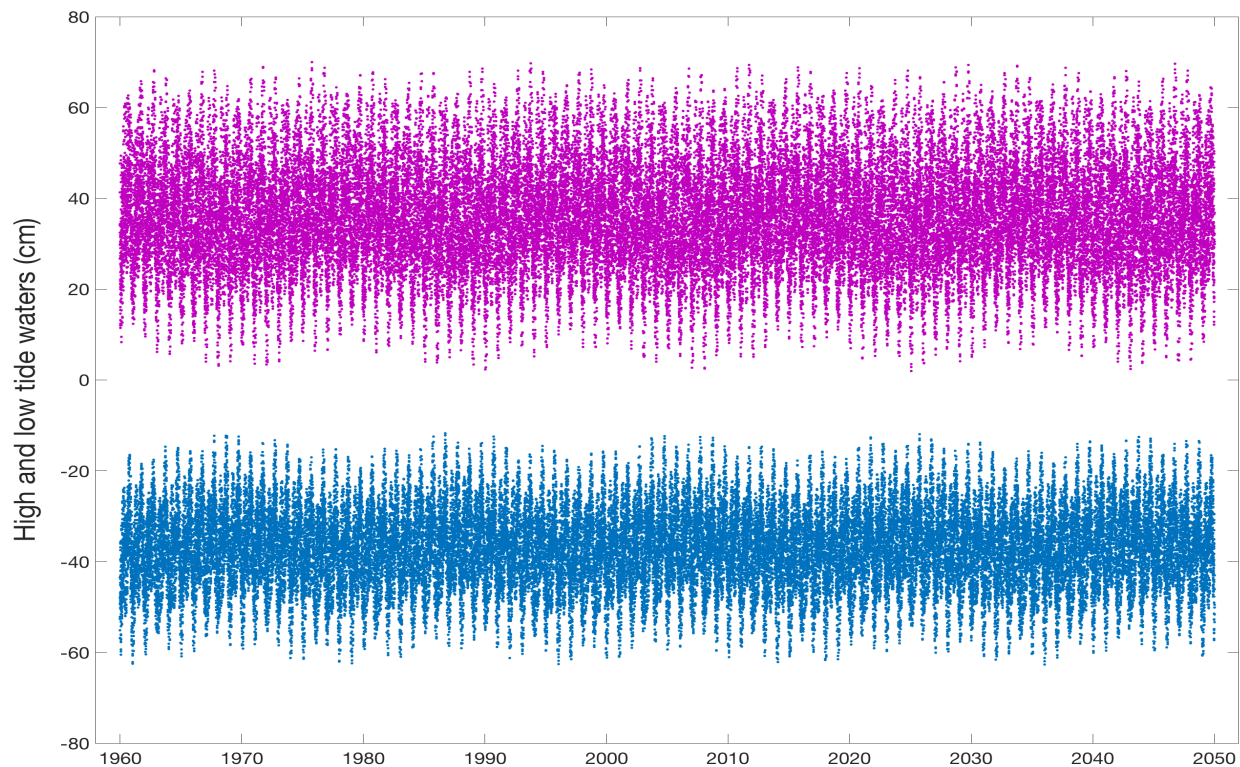


**Figure 14:** Tide observations and future estimates from 1960 - 2050. Pink- High tide. Blue- Low tide.

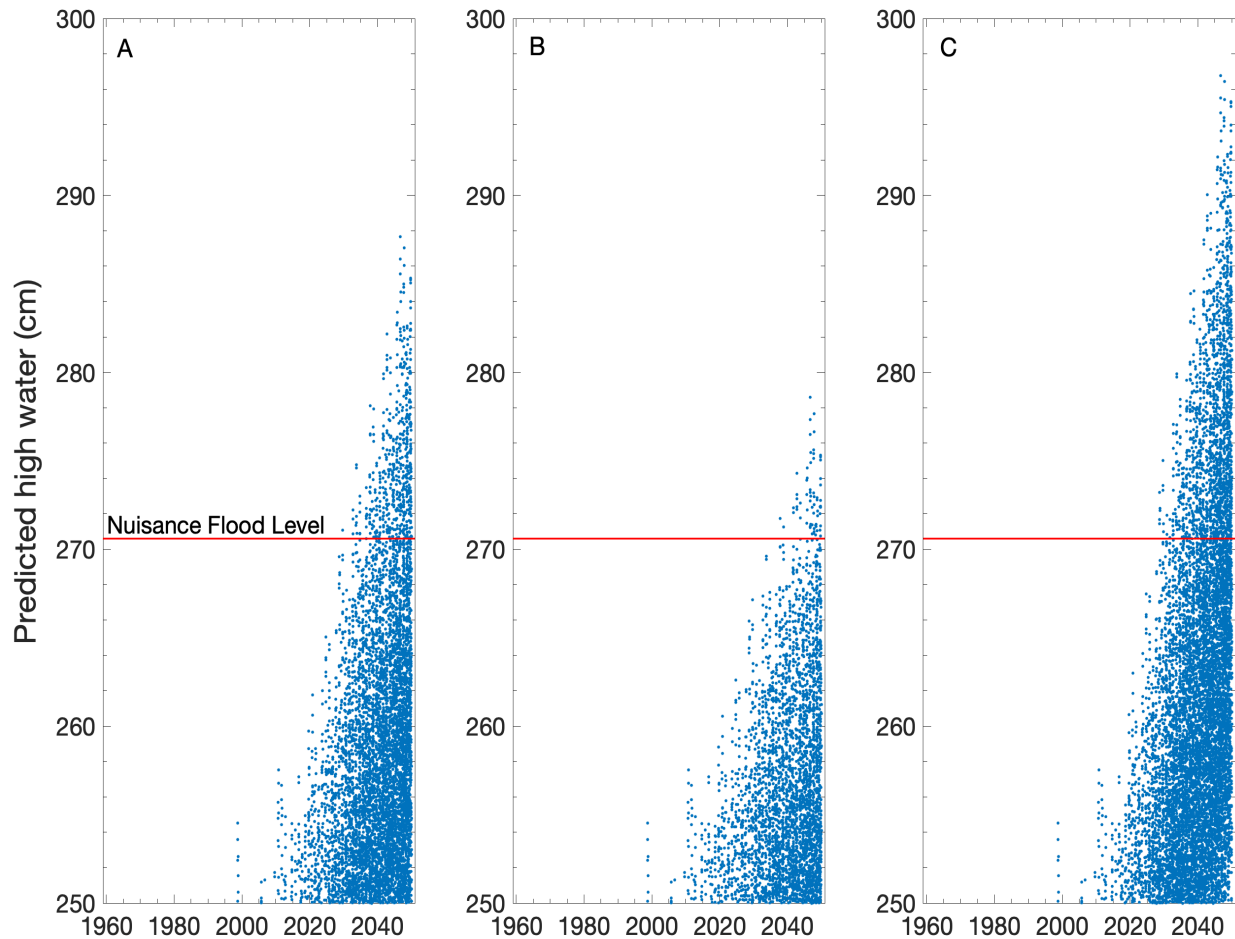


**Figure 15:** Predicted high tides exceeding the nuisance flood level of 53 cm above MHHW. A shows the medium scenario; B the low scenario; C the high scenario.

#### 4.3.2 INTERNAL CLIMATE VARIABILITY

To determine future IC, first the natural climate signals are isolated using past observations. To do this, an EMD was performed on the observed monthly sea level height data at Sewell’s Point after the annual signal was removed. This was done to prevent overlap with the tidal predictions, which included seasonal cycles. As explained in the previous chapter, the EMD acts as a suite of band-pass filters that separates the natural climate signals into IMFs – each with its own intrinsic time-scale – without leaving the time-domain. Figure 16 shows the 8 IMFs extracted from the data, with dominant frequencies that range from high-frequency to low-frequency. We are interested in the IMFs that cover the range from annual to multi-decadal

variability (subplots 2 – 7), which will be referenced hereafter as A, B, C, D, E and F. Modes C-F (or the inter-annual to decadal data) only accounts for roughly 10% of the total variance so in this case, which differs from chapter 3, the annual signals (IMF A and B) were included because they are important to simulate the impact of natural fluctuations in sea level and thus flooding. The first and last IMF were not used because the first one shows too high of frequencies on the order of less than 1 year and may be influenced by short term wind events, and the last IMF was not used since it represents SLR and would overlap with the SLR projections.

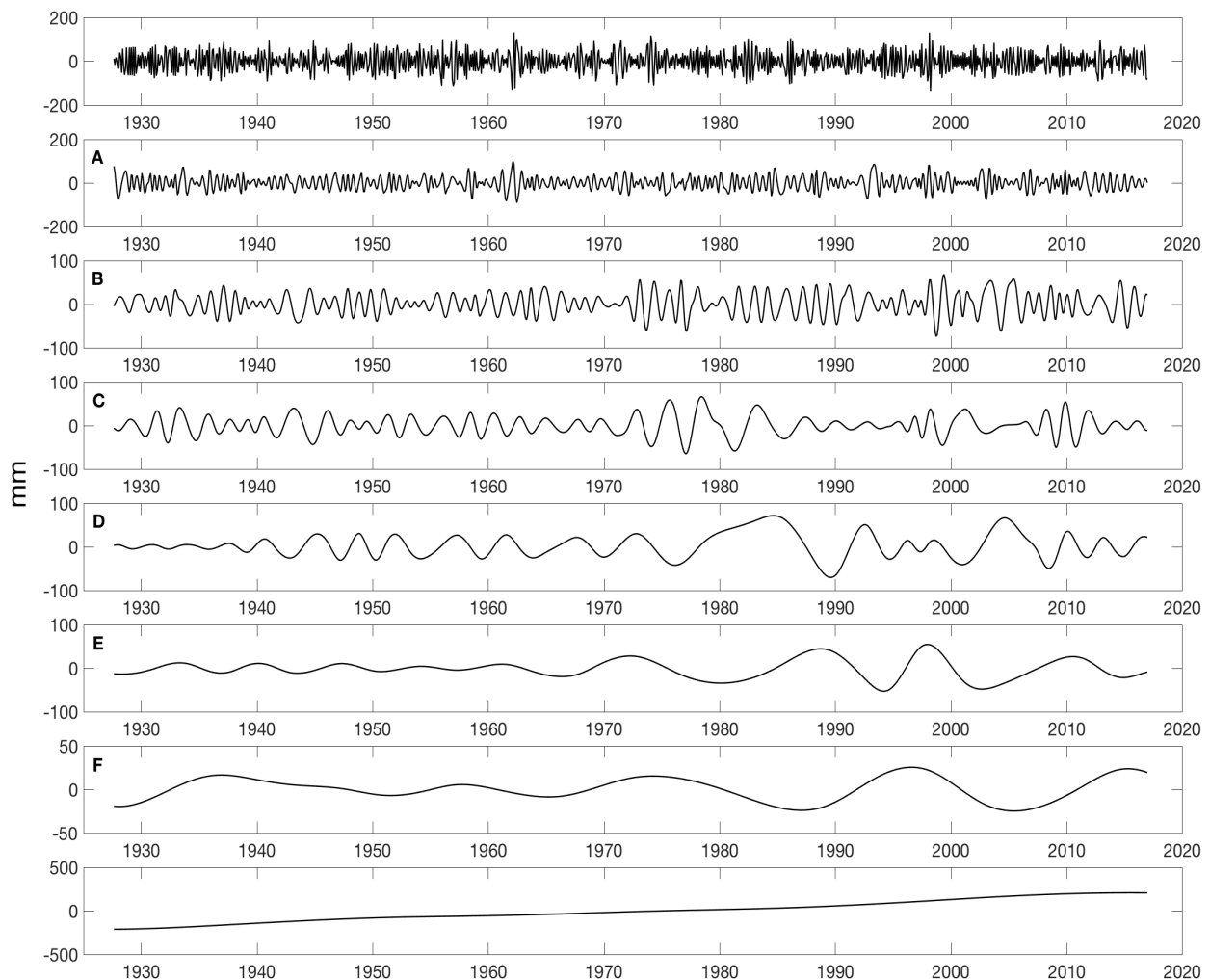


**Figure 16:** IMFs from the EMD analysis on Sewell’s Point monthly sea level data. Top three plots indicate signals on the order of annual variability. The next two show annual variability, with the two plots following on decadal time-scales. The last subplot indicates multi-decadal time-scales.

To use the selected IMFs, we assume that IC will occur in the future as it has been occurring in the past. Because we cannot conclude that the variability will repeat itself exactly, a randomization procedure is used to provide different possibilities of how these internal variabilities could be combined and applied to in the future. We are only interested in creating a new time-series of IC to apply to the future years, from January 2017 to December 2049. By determining possibilities of future IC, we can have a better idea of how nuisance flooding will progress in Norfolk from more than astronomical tides.

We extracted randomized years from the selected IMFs (A – F) to create a synthetic time-series of 33 years, which was added directly to the projected years from the three sea level scenarios plus the tidal predictions. To capture potential phasing of the signals in the IMFs, different window lengths were extracted from each mode. More specifically, in IMF A, B, and C, random 5-year segments were taken out of the IMFs to create new 33-year long time-series. The remaining IMFs had a similar process done with 10, 15, and 20 year segments removed from D, E, and F, respectively. These 5 to twenty-year time segments were chosen based off of the IMF frequencies occurring on those time-scales as seen in Figure 16. With the new randomized time segments from all 6 IMFs, they were added together, smoothed to remove discontinuities, and the mean subtracted. This time series now represents possible natural internal sea level height variability on the order of annual to decadal time-scales. 10,000 randomizations of this process were created, then each one was added on to the future years of the low, medium, and high projection with the tides. This gives us 10,000 iterations of potential nuisance flooding scenarios for each SLR case, which included the tidal and IC influences.

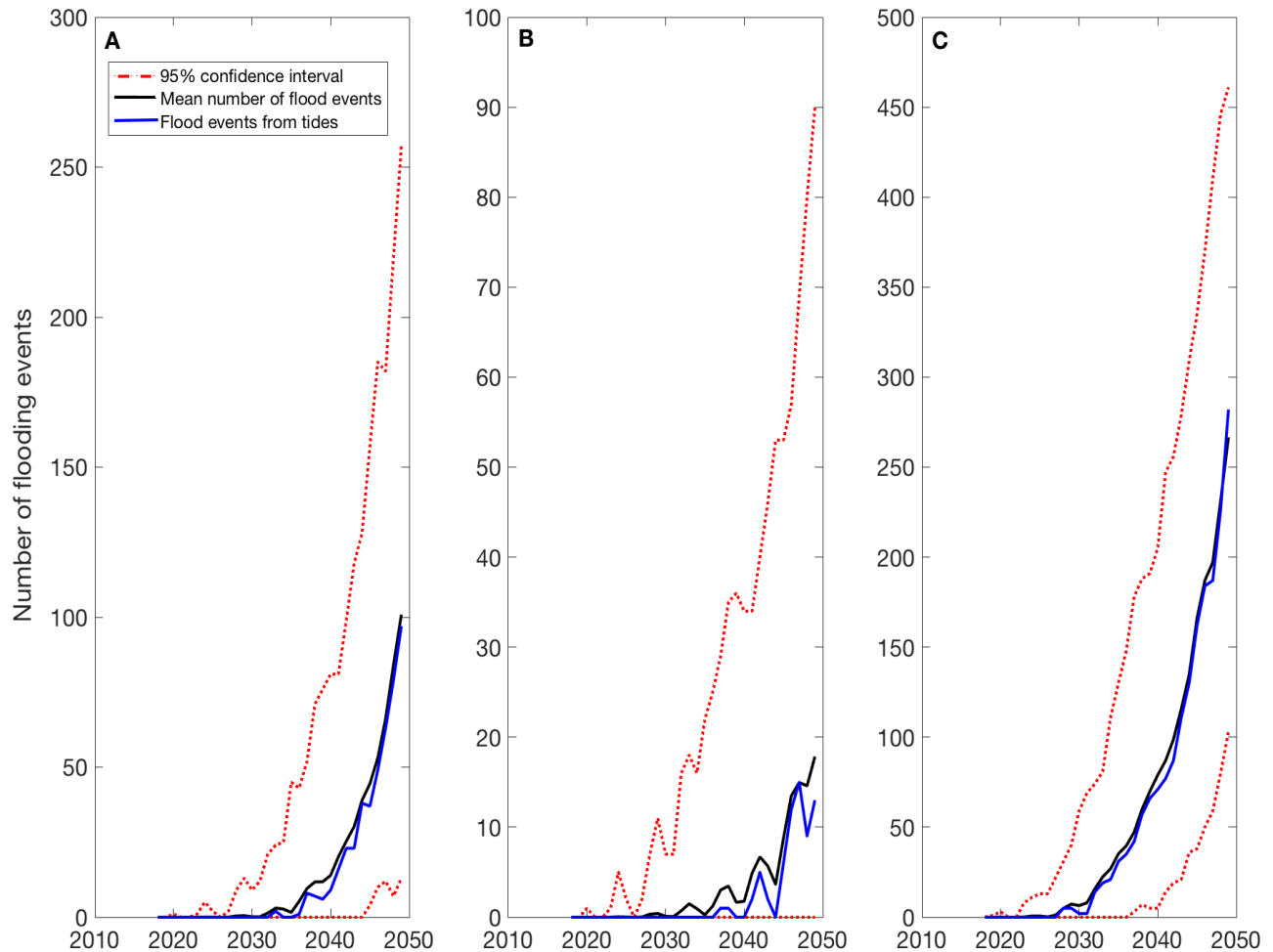
#### 4.4 RESULTS

Figure 15 shows the flooding events for the three different SLR cases plus tides. An event is defined here as when the predicted high water exceeds the nuisance flood level. Each event will be relatively short, on the order of minutes (if the predicted high water barely exceeds the nuisance flood level) to a few hours [Ray and Foster, 2016]. This is because low tide will occur roughly 6 hours after high tide, and soon brings the water level back down under the nuisance flooding threshold. From this analysis, no nuisance flood events are expected from tides alone

until around 2030 for all 3 scenarios. This is the case because although nuisance flood events have already been occurring in Norfolk, (11 flood days recorded in 2016 [*Sweet et al.*, 2017]) they happen on a daily time-scale in conjunction with other high-frequency events like storms or high wind events, which were removed by using the annual sea level data as discussed previously. Figure 15 shows the medium scenario with a total of 458 events throughout the time period, with the first event occurring in 2030. On the low and high end, these scenarios show 66 and 1816 total events, respectively. It is clear that the number of events relies heavily on how SLR will progress in the future, and the number of flood events for each scenario is still likely to change due to wind driven events. Also, IC can temporarily increase or decrease regional RSLR, shifting that baseline for high-frequency events to act upon. It is important to realize that IC can either increase or decrease the number of flood events as it lowers or raises sea level.

The results from combining the three different SLR scenarios plus the tides and different combinations of potential IC are depicted in Figure 17. Averaging the number of flood events across all 10,000 iterations (black line) provides an estimate of how many events could be expected per year. This is very close to the tides alone analysis (blue line) due to IC essentially being averaged out when looking at the mean events. The red dashed line shows the 95% confidence interval of the mean black line. The medium scenario gives an average total of 579 events across the time-frame (2018 – 2050), the low scenario yielded an average of 140 events and the high scenario showed 1992 events. By using a randomization procedure to include IC in the flood estimates, the average number of flood events for each scenario changes slightly with each new iteration. However, the average number of events stays within a few events of the numbers presented here each time. Compared to the flooding with tides alone, including IC into the analysis increased the number of events in the low scenario by 212%, medium scenario by 126%, and high scenario by 110%. Furthermore, and importantly for planning, each scenario in Figure 17 shows a relatively large confidence interval resulting from the possible range of IC. For example, the low scenario has a potential to have 0 nuisance flood events by 2050, or upwards of 60 events within the 95% confidence interval. Similarly, the upper end of the high scenario confidence interval is over 450 events by 2050. While the exact timing is unknown, at

some point in the future, periods of elevated sea level due to IC will occur, leading to Norfolk experiencing the number of flood events at the higher end of the confidence bound.



**Figure 17:** Average number of flood events each year across the 10,000 iterations combining tides, IC, and SLR scenarios in black. 95% confidence estimates on this mean are in dashed red. The number of nuisance flood events from tidal influences alone are in blue. A shows the medium scenario; B the low scenario; C the high scenario.

## CHAPTER 5

### DISCUSSION AND CONCLUSIONS

#### 5.1 OVERVIEW

Sea level rise, and the resulting consequences, is not uniform since regional sea level can deviate greatly from the global mean. It is critical to understand how each coastal city is going to be currently affected from the rising waters, along with in the future. Satellite altimeters have provided detailed regional sea level measurements, but with the short record it is difficult to create future projections. With 20<sup>th</sup> century sea level data, the satellite record can be put into context and higher quality future regional sea level projections can be created by determining accelerations. From this knowledge, in chapter 2, a 20<sup>th</sup> century sea level trend map was created. One map shows regional trends including internal climate variability with the help of CMIP5 models, and with the internal climate variability removed, an anthropogenic map was isolated providing trends from mass changes and thermal expansion. Also, individual contributions to GMSL from different melt sources, groundwater withdrawal and water impoundment were quantified.

In the future, it is not only the continual effects from anthropogenic forcings that will contribute to changing sea level, but also natural internal climate variability. This is a key piece to include for future sea level estimates, as internal events may either suppress or enhance sea level. In chapter 3, future sea level was estimated along the United States East and West coast by taking into account sea level trends from anthropogenic forces and estimates of internal climate variability.

Lastly, understanding how sea level could possibly change in the future is critical for emergency managers and coastal planners. With increasing sea level, high frequency events such as tides and storms pose more of a threat to coastal cities as they act upon the base sea level height. Suddenly high tides can start inundating roads when it never did before leading to nuisance flooding. Future high tide flooding was analyzed for Norfolk, Virginia in chapter 4

taking into account tides and tides coupled with internal climate variability on top of three sea level rise scenarios.

## 5.2 DISCUSSION

### 5.2.1 20<sup>TH</sup> CENTURY SEA LEVEL RISE

There have been very few comprehensive studies on past RSLR and determining the true regional sea level over the 20<sup>th</sup> century is a difficult process, especially with the limited data and lack of additional independent data to verify these results.

There are caveats with this trend map, mainly in the fact that it is built from only 15 tide gauges. Although these gauges are thought to be of the highest quality, the results may differ if a different subset of gauges are used. While looking at more TG's to include in the estimated trends might appear to be useful, many gauges do not even span the full centennial time-scale, and many suffer from large vertical displacements that would be difficult to correct. As previously touched upon, using GPS corrections for the selected TG's introduces a large spread in the estimated trends (results not shown), and so other gauges with vertical displacement cannot reliably be used even if they meet the length requirement. TG records that are affected by unresolved internal variability or vertical displacement that cannot be corrected, significantly impact the long-term GMSL trend [*Hamlington and Thompson, 2015*], making it critical to choose appropriate TG's. The supplementary material in *Thompson et al. [2016]* discusses several other gauges in detail and the reason for excluding them. It should also be noted that these gauges are heavily clustered in the Northern hemisphere, and no correction or assumptions for that fact was taken into account.

The 15 TG's used in this study do underestimate the positive contribution from 5 of the 7 ice melt fingerprints, along with the groundwater withdrawal contribution, and overestimate the negative contribution from water impoundment. It should be noted that this study is built off of several current estimates, that do not have historical context. The ice melt, ground water withdrawal, and water impoundment are all based on current measurements. The ice for example is taken from GRACE satellite over the years 2003 - 2015. The assumption here is that the current trends can be applied to the past, which may ultimately lead to uncertainties.



It is also worth mentioning that the GMSL trend obtained ( $1.59 \pm 0.40$ ) is larger than other recently published works covering a similar time frame [*Dangendorf et al.*, 2017; *Hay et al.*, 2015]. To obtain a GMSL more in line with the other studies, the most likely explanations are that the TG's are either significantly impacted by non-GIA subsidence, or the average GIA contribution is significantly underestimated.

Even with these caveats, this study represents a novel and comprehensive approach to determining regional sea level during the 20<sup>th</sup> century. The maps and data created can serve as a foundation for other researchers to work off of to create more robust studies to potentially validate this work, along with using the data for future SLR estimates.

## 5.2.2 FUTURE SEA LEVEL RISE ON THE EAST AND WEST U.S. COAST

There has been numerous studies to determine future SLR along coastal towns [*Boon et al.*, 2018; *Han et al.*, 2016; *Kopp et al.*, 2014; *Perrette et al.*, 2012; *Strauss* 2013; *Sweet et al.*, 2017; *Telbaldi et al.*, 2012]. Many of these works use several datasets such as ice melt, thermal expansion, and subsidence rates to determine future projections, where the basis of many of these works relies on TG data. An important component to increasing sea level is internal climate variability and it is necessary to know how this will affect future SLR rates. The TG network as discussed has many issues, and does not provide a comprehensive range of data along the entire coastline. To determine future internal climate variability, the AVISO satellite data is used instead, allowing for a method to be independent of the TG network. Even with the discrepancies of using satellite altimetry near the coast, this is the best method so far to get away from the variable TG network and provide continuous data along the coastline.

The resulting maps only provide a potential range of SLR relative to 2016. There are still discrepancies with using the AVISO data and the anthropogenic trend map. By only taking linear trends from the 20<sup>th</sup> century map, we are ignoring any accelerations that have been occurring in the sea level record. At Sewell's Point for example, it was shown from the TG (Figure 13) that from 1928 - 2016 there is a 4.6 mm/yr SLR, but according to Figure 7A there is a trend of around 1.7 mm/yr near the Virginia coast (around 1.6 mm/yr in Figure 8 if disregarding internal variability). This smaller trend is what was extended out for the projections, which clearly

disregards any acceleration, and assumes to be representative of coastal data even with the coarse resolution.

It is important to note also that several coastal cells in Figure 11 and 12 that are adjacent to each other may have different values. In reality there would not be such a large deviation in sea level for coastal areas right next to each other, and this arises due to the EMD process. The AVISO data varies from cell to cell, and these variations are clearly shown through the IMFs. With the randomization procedure, and the minimum and maximum values chosen, this results in some cells next to each other to significantly deviate from one another, although this would not happen in actuality.

Although a comparison was made between the resulting maximum maps and other studies, this type of comparison is difficult and rough. By using the coarse anthropogenic sea level trends, and AVISO data, the resulting sea level estimates are not completely applicable to the coastline as larger signals are expected. The minimum and maximum trend maps show a robust range of possibilities of how internal climate variability could enhance or suppress regional SLR in addition to other factors. The minimum sea level map, although highly improbable, still provides valuable information for how these climate events can theoretically combine in such a way as to promote a decrease in sea level. With a linear trend and the maximum combined internal variability, these estimates still fall short of what is being reported by other sources, especially along the East coast. The maximum sea level maps for both years (especially 2050), should be looked at as bare-minimum sea level estimates, and higher amounts of SLR should be expected for the future due to sea level rise acceleration [*Boon, 2012; Church & White, 2006; Houston & Dean, 2011; Jevrejeva et al., 2008, 2014; Kenigson & Han, 2014*].

### 5.2.3 NUISANCE FLOODING IN NORFOLK, VIRGINIA

Nuisance flooding will increase along coastal towns as sea level continues to rise. Norfolk in the Hampton roads region is particularly prone to flooding due to its low elevation, with over a million people and the world's largest navy base at risk. The frequency and severity of future flooding will be heavily influenced by how much SLR occurs in the future. There has yet to be seen a purely tide-induced nuisance flood event in Norfolk, with that expecting to

change around 2030 across all sea level scenarios. Tides are not going to be the only factor to consider, and it is important to keep in mind that these flooding events generally occur when several processes converge, such as SLR combined with wind-driven events like coastal storms. These are virtually impossible to spatially and temporally predict, even though we know that they will occur at some point in the future. IC is also difficult to predict, and although we cannot forecast exact phasing, we can describe how it might impact flood events in the future based on past observations. With internal climate variability added in, the time frame shifts such that nuisance flood events occur earlier than 2030 from the combination of SLR, tides, and IC. These results show that flooding will increase without the occurrence of a storm or a short-term wind driven event. With these other high-frequency events, the number of nuisance flooding days will only be higher in the future for Norfolk. The flooding events presented here, especially in the medium to high end, should be taken as a baseline for coastal planners looking into the future as wind-driven events will increase the severity and number of flood days beyond what is presented here.

### 5.3 CONCLUSIONS

Sea level rise presents a problem that coastal managers and policy makers are not confident how to plan for. Several mitigation and adaptation plans have already been implemented in coastal towns such as raising homes, employing sea walls and living shorelines, and moving landward. By understanding how the oceans have been varying regionally, this sets up researchers to create better projections of sea level rise to be applied to each coastal city, who will need their own adaptation and mitigation plans as the ocean affects them differently. Throughout these chapters it has been illustrated that sea level is continuing to rise, which will lead to consequences like nuisance flooding. Although there are caveats in the methods presented throughout here, the results from each chapter provides critical information going forward in the study of sea level rise. Especially the methods/results in chapters 2 and 3, these act as frameworks for historical and future predictions of regional sea level, and are foundations to be expanded upon. Chapter 4 provides some of the more sobering details of nuisance flooding in Norfolk as sea level, tides, and natural internal climate variability act in a way to potentially

cause minor flooding for the majority of the year by 2050. Going forward, sea level rise will continually be a crucial result of climate change that needs further studying, and for researchers and coastal planners to work together to create sound policies to protect coastal communities.

## REFERENCES

- Adhikari, S., Ivins, E.R., & Larour, E. (2016). ISSM-SESAW v1.0: mesh-based computation of gravitationally consistent sea-level and geodetic signatures caused by cryosphere and climate driven mass change. *Geoscientific Model Development*, 9(3), 1087-1109. <https://doi.org/10.5194/gmd-9-1087-2016>.
- Boening, C., Willis, J., Landerer, F., Nerem, S., & Fasullo, J. (2012). The 2011 La Niña: So Strong, the oceans fell. *Geophysical Research Letters*, 39, L19602. <https://doi.org/10.1029/2012GL053055>.
- Boon, J.D., Mitchell, M., Loftis, J.D., & Malmquist, D.M. (2018). Anthropocene sea level change: A history of recent trends in the U.S. East, Gulf, and West coast regions. Special report in Applied Marine Science and Ocean Engineering (SRAMSOE) No. 467. *Virginia Institute of Marine Science, College of William and Mary*. <https://doi.org/10.21220/V5T17T>.
- Boon, J.D. (2012). Evidence of sea level acceleration at U.S. and Canadian tide stations, Atlantic coast, North America. *Journal of Coastal Research*. 28(6), 1437-1445. <https://doi.org/10.2112/JCOASTRES-D-12-00102.1>
- Caron, L., Métivier, L., Greff-Lefftz, M., Fleitout, L. & Rouby, H. (2017). Inverting Glacial Isostatic Adjustment signal using Bayesian framework and two linearly relaxing rheologies, *Geophysical Journal International*, 209(2), 1126–1147.
- Carson, M., Köhl, A., & Stammer, D. (2015). The impact of regional multidecadal and century-scale internal climate variability on sea level trends in CMIP5 models. *Journal of Climate*, 28, 853 -861. <https://doi.org/10.1175/JCLI-D-14-00359.1>.
- Chambers, D.P. (2015). Evaluation of empirical mode decomposition for quantifying multi-decadal variations and acceleration in sea level records. *Nonlinear Processes in Geophysics*, 22, 157-166. <https://doi.org/10.5194/npg-22-157-2015>.
- Cheng, Y., Ezer, T., Atkinson, L., & Xu, Q. (2017). Analysis of tidal amplitude changes using the EMD method. *Continental Shelf Research*, 148, 44-52. <https://doi.org/10.1016/j.csr.2017.09.009>.
- Church, J.A., & White, N. J. (2006). A 20<sup>th</sup> century acceleration in global sea-level rise. *Geophysical Research Letters*, 33, L01602. <https://doi.org/10.1029/2005GL024826>.

- Church, J.A., & White, N. J. (2004). Estimates of the regional distribution of sea level rise over the 1950-2000 period. *American Meteorological Society*, 17, 2609-2625.
- Church, J.A., & White, N. J. (2011). Sea-Level rise from the late 19<sup>th</sup> to the Early 21<sup>st</sup> century. *Surveys in Geophysics*, 32, 585-602. <https://doi:10.1007/s10712-011-9119-1>.
- Church, J. A., Clark, P. U., Cazenave, A., Gregory, J. M., Jevrejeva, S., Levermann, A., et al. (2013). Sea level change. In Stocker, T. F., et al., *Climate change 2013: The physical science basis. Contribution of working group I to the fifth assessment report of the intergovernmental panel on climate change*. Cambridge, UK and New York, NY: Cambridge University Press.
- Cipollini, P. Calafat, F.M., Jevrejeva, S., Melet, A., & Prandi, P. (2017). Monitoring sea level in the coastal zone with satellite altimetry and tide gauges. *Surveys in Geophysics*, 38, 33-57. <https://doi:10.1007/s10712-016-9392-0>.
- Dahl, K., Fitzpatrick, M., & Spanger-Siegfried, E. (2017). Sea level rise drives increased tidal flooding frequency at tide gauges along the U.S. East and Gulf Coasts: Projections for 2030 and 2045. *PLoS ONE*, 12(2). E0170949. <https://doi.org/10.1371/journal.pone.0170949>.
- Dangendorf, S., Marcos, M., Wöppelmann, G., Conrad, C., Frederikse, T., & Riva, R. (2017). Reassessment of 20<sup>th</sup> century global mean sea level rise. *PNAS*, 114(23), 5946-5951. <https://doi:10.1073/pnas.1616007114>.
- Ezer, T. (2013). Sea level rise, spatially uneven and temporally unsteady: Why the U.S. East Coast, the global tide gauge record, and the global altimeter data show different trends. *Geophysical Research Letters*, 40, 5439–5444. <https://doi:10.1002/2013GL057952>.
- Ezer, T. (2016). Can the Gulf Stream induce coherent short-term fluctuations in sea level along the U.S. East Coast?: A modeling study. *Ocean Dynamics*, 66(2), 207-220. <https://doi:10.1007/s10236-016-0928-0>.
- Ezer, T. (2017). A modeling study of the role that bottom topography plays in Gulf Stream dynamics and in influencing the tilt of mean sea level along the U.S. East Coast. *Ocean Dynamics*, 67(5), 651-664. <https://doi:10.1007/s10236-017-1052-5>.
- Ezer, T., & Atkinson, L.P. (2014). Accelerated flooding along the U.S. East Coast: On the impact of sea-level rise, tides, storms, the Gulf Stream, and the North Atlantic Oscillations. *Earth's Future*, 2(8), 362-382. <https://doi:10.1002/2014EF000252>.

- Ezer, T., & Atkinson, L.P. (2017). On the predictability of high water level along the U.S. East Coast: can the Florida Current measurement be an indicator for flooding caused by remote forcing?. *Ocean Dynamics*, 67(6), 751-766. <https://doi.org/10.1007/s10236-017-1057-0>.
- Ezer, T., Atkinson, L.P., Corlett, W.B., & Blanco, J.L. (2013). Gulf Stream's induced sea level rise and variability along the U.S. mid-Atlantic coast. *Journal of Geophysical Research*, 118, 685–697. <https://doi.org/10.1002/jgrc.20091>
- Ezer, T., Haigh, I.D., & Woodworth, P.L. (2016). Nonlinear sea-level trends and long-term variability on western European coasts. *Journal of Coastal Research*, 32(4), 744-755. <https://doi.org/10.2112/JCOASTRES-D-15-00165.1>.
- Flick, R.E., Murray, J., & Ewing, L. (2003). Trends in United States tidal datum statistics and tide range. *Journal of Waterway Port Coastal and Ocean Engineering*, 129(4), 155-164. [http://doi.org/10.1061/\(ASCE\)0733-950X\(2003\)129:4\(155\)](http://doi.org/10.1061/(ASCE)0733-950X(2003)129:4(155)).
- Gregory, J. M., White, N. J., Church, J. A., Bierkens, M. F. P., Box, J. E., van den Broeke, M. R., et al. (2013). Twentieth-century global-mean sea level rise: Is the whole greater than the sum of the parts? *Journal of Climate*, 26(13), 4476–4499. <https://doi.org/10.1175/JCLI-D-12-00319.1>.
- Hamlington, B.D., Leben, R.R., Nerem, R.S., Han, W., & Kim, K.Y. (2011). Reconstructing sea level using cyclostationary empirical orthogonal functions. *Journal of Geophysical Research*, 116, C12015. <https://doi.org/10.1029/2011JC007529>.
- Hamlington, B.D., Leben, R., Strassburg, M., Merem, R., & Kim, K. (2013). Contribution of the Pacific Decadal Oscillation to global mean sea level trends. *Geophysical Research Letters*, 40, 5171-5175. <https://doi.org/10.1002/grl.50950>.
- Hamlington, B. D., Leben, R. R., Kim, K.-Y., Nerem, R. S., Atkinson, L. P., & Thompson, P. R. (2015). The effect of the El Niño-Southern Oscillation on U.S. regional and coastal sea level, *Journal of Geophysical Research: Oceans*, 120, 3970– 3986. [https://doi: 10.1002/2014JC010602](https://doi.org/10.1002/2014JC010602).
- Hamlington, B. D., & Thompson, P.R. (2015). Considerations for estimating the 20<sup>th</sup> century trend in global mean sea level. *Geophysical Research Letters*, 42(10). [https://doi: 10.1002/2015GL064177](https://doi.org/10.1002/2015GL064177).
- Hamlington, B. D., Cheon, S. H., Thompson, P. R., Merrifield, M. A., Nerem, R. S., Leben, R. R., & Kim, K-Y. (2016a). An Ongoing Shift in Pacific Ocean Sea Level. *Journal of*

- Geophysical Research: Oceans*, 121(7), 5084 – 5097. [https://doi:10.1002/2016JC011815](https://doi.org/10.1002/2016JC011815).
- Hamlington, B.D., Thompson, P., Hammond, W.C., Blewitt, G., & Ray, R.D. (2016b). Assessing the impact of vertical land motion on twentieth century global mean sea level estimates. *Journal of Geophysical Research*, 121, 4980–4993.
- Han, W., Meehl, G.A., Hu, A., Alexander, M., Yamagata, T., Yuan, D., et al. (2013). Intensification of decadal and multi-decadal sea level variability in the western tropical Pacific during recent decades. *Climate Dynamics*, 43(5-6), 1357-1379. [https://doi:10.1007/s00382-013-1951-1](https://doi.org/10.1007/s00382-013-1951-1).
- Han, W., Meehl, G.A., Stammer, D., Hu, A., Hamlington, B.D., Kenisgon, J., Palanisamy, H., & Thompson, P. (2016). Spatial patterns of sea level variability associated with natural internal climate modes. *Surveys in Geophysics*, 38, 217-250. [https://doi:10.1007/s10712-016-9386-y](https://doi.org/10.1007/s10712-016-9386-y).
- Hay, C.C., Morrow, E., Kopp, R., & Mitrovica, J.X. (2015). Probabilistic reanalysis of twentieth-century sea-level rise. *Nature*. 517(7535), 481-484. [https://doi:10.1038/nature14093](https://doi.org/10.1038/nature14093).
- Houston, J.R., Dean, R.G. (2011). Sea-Level accelerations based on U.S. tide gauges and extensions of previous global-gauge analyses. *Journal of Coastal Research*. 27(3), 409-417, <https://doi.org/10.2112/JCOASTRES-D-10-00157.1>
- Hu, A., & Deser, C. (2013). Uncertainty in future regional sea level rise due to internal climate variability. *Geophysical Research Letters*, 40, 2768-2772. [https://doi:10.1002/grl.50531](https://doi.org/10.1002/grl.50531).
- Huybrechts, P., Goelzer, H., Janssens, I., Driesschaert, E., Fichefet, T., Goosse, H., & Loutre, M. F. (2011). Response of the Greenland and Antarctic ice sheets to multi-millennial greenhouse warming in the Earth system model of intermediate complexity LOVECLIM. *Surveys in Geophysics*, 32(4–5), 397–416. <https://doi.org/10.1007/s10712-011-9131-5>.
- Jevrejeva, S., Moore, J.C., Grinsted, A., & Woodworth, P.L. (2008). Recent global sea level acceleration started over 200 years ago? *Geophysical Research Letters*, 35(8). L08715. [https://doi:10.1029/2008GL033611](https://doi.org/10.1029/2008GL033611).
- Jevrejeva, S., Moore, J.C., Grinsted, A., Matthews, A.P., & Spada, G. (2014). Trends and acceleration in global and regional sea levels since 1807. *Global and Planetary Change*, 113, 11-22. <https://doi.org/10.1016/j.gloplacha.2013.12.004>.



- Kenigson, J.S., & Han, W. (2014). Detecting and understanding the accelerated sea level rise along the east coast of the United States during recent decades. *Journal of Geophysical Research: Oceans*, 119(12), 8749-8766. <https://doi.org/10.1002/2014JC010305>.
- Kleinosky, L.R., Yarnal, B., & Fisher, A. (2007). Vulnerability of Hampton Roads, Virginia to storm-surge flooding and sea level rise. *Natural Hazards*, 43-70. <https://doi:10.1007/s11069-006-0004-z>.
- Kopp, R.E., Horton, R.M., Little, C.M., Mitrovica, J.X., Oppenheimer, M., Rasmussen, D.J., et al. (2014). Probabilistic 21st and 22nd century sea-level projections at a global network of tide-gauge sites. *Earth's Future*, 2(8), 383-406. <https://doi.org/10.1002/2014EF000239>.
- Lehner, B., Reidy Liermann, C., Revenga, C., Vörösmarty, C., Fekete, B., Crouzet, P., et al. (2011). High-Resolution Mapping of the World's Reservoirs and Dams for Sustainable River-Flow Management. *Frontiers in Ecology and the Environment*, 9(9), 494-502. <https://doi.org/10.1890/100125>.
- Marcos, M., Marzeion, B., Dangendorf, S., Slangen, A.B.A., Palanisamy, H., & Fenoglio-Marc, L. (2016). Internal variability versus anthropogenic forcing on sea level and its components. *Surveys in Geophysics*, 38(1), 329-348. <https://10.1007/s10712-016-9373-3>.
- Merrifield, M.A., Thompson, P.R., & Lander, M. (2012). Multidecadal sea level anomalies and trends in the western tropical Pacific. *Geophysical Research Letters*, 39, L13602. <https://doi:10.1029/2012GL052032>.
- Moftakhari, H. R., AghaKouchak, A., Sanders, B. F., Feldman, D. L., Sweet, W., Matthew, R. A., & Luke, A. (2015). Increased nuisance flooding along the coasts of the United States due to sea level rise: Past and future, *Geophysical Research Letters*, 42, 9846-9852. <https://doi:10.1002/2015GL066072>.
- Molla, K.I., Rahman, S.M., Sumi, A., & Banik, P. (2005). Empirical mode decomposition analysis of climate changes with special reference to rainfall data. *Discrete Dynamics in Nature and Society*. <https://doi:10.1155/DDNS/2006/45348>.
- NASA JPL. (2013). Long-running Jason-1 ocean satellite takes final bow. <https://www.jpl.nasa.gov/news/news.php?release=2013-213>
- NOAA. (2017). Shallow Coastal Flooding (Nuisance Flooding). U.S. Climate Resilience Toolkit. <https://toolkit.climate.gov/topics/coastal-flood-risk/shallow-coastal-flooding- nuisance-flooding>.

- NOAA Tides & Currents. (2018). Datums for 8638610, Sewells Point VA. <https://tidesandcurrents.noaa.gov/datums.html?id=8638610>
- Perrette, M., Landerer, F., Riva, R., Frieler, K., & Meinshausen, M. (2012). Probabilistic projection of sea-level change along the world's coastlines. *Earth System Dynamics Discussions*, 3, 357-389. <https://doi:10.5194/esdd-3-357-2012>.
- Piecuch, C., Dangendorf, S., Ponte, R., & Marcos, M. (2016). Annual Sea Level Changes on the North American Northeast Coast: Influence of local winds and barotropic motions. *American Meteorological Society*. <https://doi.org/10.1175/JCLI-D-16-0048.1>.
- Piecuch, C.G., & Ponte, R.M. (2015). Inverted barometer contributions to recent sea level changes along the northeast coast of North America. *Geophysical Research Letters*, 42, 5918-5925. <https://doi/10.1002/2015GL064580>.
- Ray, R. D., & Douglas, B. C. (2011). Experiments in reconstructing twentieth-century sea levels. *Progress in Oceanography*, 91(4), 496-515. <https://doi:10.1016/j.pocean.2011.07.021>.
- Ray, R. D., & Foster, G. (2016). Future nuisance flooding at Boston caused by astronomical tides alone. *Earth's Future*, 4, 578–587. <https://doi:10.1002/2016EF000423>.
- Strauss, B. (2013). Rapid accumulation of committed sea-level rise from global warming. *PNAS Commentary*, 110(34), 13699-13700.
- Sweet, W.V., & Park, J. (2014). From the extreme to the mean: Acceleration and tipping points of coastal inundation from sea level rise. *Earth's Future*, 2(12), 579-600.
- Sweet, W.V., Park, J., Marra, J., Zervas, C., & Gill, S. (2014). Sea level rise and nuisance flood frequency changes around the United States. NOAA Technical Report NOS CO-OPS 073.
- Sweet, W.V., Kopp, R.E., Weaver, C.P., Obeysekera, J., Horton, R.M., Thieler, E.R., & Zervas, C. (2017). Global and regional sea level rise scenarios for the United States. NOAA Technical Report NOS CO-OPS 083.
- Sweet, W.V., Mara, J.J., & Dusek, G. (2017). 2016 state of U.S. high tide flooding and a 2017 outlook. Supplement to *State of the Climate: National Overview for May 2017*, published online June 2017, [https://www.ncdc.noaa.gov/monitoring-content/sotc/national/2017/may/2016\\_StateofHighTideFlooding.pdf](https://www.ncdc.noaa.gov/monitoring-content/sotc/national/2017/may/2016_StateofHighTideFlooding.pdf)

- Tebaldi, C., Strauss, B.H., & Zervas, C.E. (2012). Modelling sea level rise impacts on storms surges along US coasts. *Environmental Research Letters*, 7. [https://doi:10.1088/1748-9326/7/1/014032](https://doi.org/10.1088/1748-9326/7/1/014032).
- Thompson, P.R., Hamlington, B.D., Landerer, F.W., & Adhikari, S. (2016). Are long tide gauge records in the wrong place to measure global sea level rise? *Geophysical Research Letters*, 43(19), 403-411. [https://doi:10.1002/2016GL070552](https://doi.org/10.1002/2016GL070552).
- Vandenberg-Rodes, A., Moftakhari, H.R., AghaKouchak, A., Shahbaba, B., Sanders, B.F., & Matthew, R.A. (2016). Projecting nuisance flooding in a warming climate using generalized linear models and Gaussian processes. *Journal of Geophysical Research: Oceans*, 121, 8008-8020. [https://doi:10.1002/2016JC012084](https://doi.org/10.1002/2016JC012084).
- Vaughan, D. G., Comiso, J. C., Allison, I., Carrasco, J., Kaser, G., Kwok, R., et al. (2013). Observations: Cryosphere. In Stocker, T. F., et al. (Eds.), *Climate change 2013: The physical science basis. Contribution of working group I to the fifth assessment report of the intergovernmental panel on climate change*. Cambridge, UK and New York, NY: Cambridge University Press.
- Vinogradov, S.V., & Ponte, R.M. (2011). Low-frequency variability in coastal sea level from tide gauges and altimetry. *Journal of Geophysical Research*, 116, C07006. [https://doi:10.1029/2011JC007034](https://doi.org/10.1029/2011JC007034)
- Vitousek, S., Barnard, P.L., Fletcher, C.H., Frazer, N., Erikson, L., & Storlazzi, C.D. (2017). Doubling of coastal flooding frequency within decades due to sea-level rise. *Nature, Scientific Reports*, 7. [https://doi:10.1038/s41598-017-01362-7](https://doi.org/10.1038/s41598-017-01362-7).
- Wada, Y., VanBeek, L. P. H., Sperna Weiland, F. C., Chao, B. F., Wu, Y.-H., & Bierkens, M. F. P. (2012). Past and future contribution of global groundwater depletion to sea-level rise. *Geophysical Research Letters*, 39, L09402. <https://doi.org/10.1029/2012GL051230>.
- Wahl, T., & Chambers, D.P. (2016). Climate controls multidecadal variability in U.S. extreme sea level records. *Journal of Geophysical Research: Oceans*, 121, 1274-1290. [https://doi:10.1002/2015JC011057](https://doi.org/10.1002/2015JC011057).
- Woodworth, P.L. (2012). A Note on the nodal tide in sea level records. *Journal of Coastal Research*, 280, 316-323. <http://doi.org/10.2112/JCOASTRES-D-11A-00023.1>.
- Wöppelmann, G., & Marcos, M. (2016). Vertical land motion as a key to understanding sea level change and variability. *Reviews of Geophysics*, 54, 64–92.

## VITA

Alessandra G. Burgos

Old Dominion University  
 Department of Ocean, Earth, and Atmospheric Sciences  
 Center for Coastal Physical Oceanography  
 4111 Monarch Way Norfolk, VA 23508

### EDUCATION

---

#### Master of Science

*December 2018*

Ocean and Earth Sciences

Concentration: Physical Oceanography

Old Dominion University

*Thesis: Regional Sea Level Rise Along the United States Coasts*

#### Bachelor of Science

*May 2016*

School of Environmental Sciences

Concentration: Meteorology

Rutgers University

### PUBLICATIONS

---

**Burgos, A.**, Hamlington, B.D., Thompson, P.R., Ray, R.D. (2018). Future Nuisance Flooding in Norfolk, VA from Astronomical Tides and Annual to Decadal Internal Climate Variability.

*Geophysical Research Letters*. doi: 10.1029/2018GL079572

Hamlington, B.D., **Burgos, A.**, Thompson, P.R., Landerer, F.W., Piecuch, C.G., Adhikari, S. et al. (2018). Observation-Driven Estimation of the Spatial Variability of 20<sup>th</sup> Century Sea Level Rise.

*Journal of Geophysical Research: Oceans*, 123, 2129-2140.

### PRESENTATIONS

---

2018. Trends in Regional Sea Level Rise in the 20<sup>th</sup> Century. Oral presentation at *Ocean Sciences Meeting, Spring Meeting*, Portland Oregon.

2017. Trends in Regional Sea Level Rise in the 20<sup>th</sup> Century. Poster presentation at *American Geophysical Union, Fall Meeting*, New Orleans, Louisiana.

2017. Comparison of Polar Amplification in CMIP5 against Observations. Poster presentation at *American Meteorological Society, Spring Meeting*, Seattle, Washington.